Pulsed optoacoustic spectroscopy of condensed matter

C. K. N. Patel

Bell Laboratories, Murray Hill, New Jersey 07974

A. C. Tam

IBM Research Laboratory, San Jose, California 95193

The authors discuss the theory and experiments dealing with the pulsed optoacoustic effect (i.e., generation of a transient acoustic wave by absorption of an optical pulse) in condensed matter. Their primary interest lies in the measurement of small absorption coefficients ($\ll 10^{-1}$ cm^{-1}). At present an experimental capability of measuring absorption coefficients as small as 10^{-6} cm^{-1} has been demonstrated, and further improvement is foreseen. The pulsed optoacoustic absorption measurement technique has been applied to the following linear spectroscopic studies: (1) precise measurements of the optical absorption spectra of H_2O and D_2O; (b) accurate determination of absorption strengths and profiles of high harmonics ($n = 6$, 7, and 8) of vibrational modes in transparent organic liquids (e.g., benzene); (c) quantitative absorption spectra of thin (~ 1–$10\,\mu$m) liquid films; and (d) quantitative absorption spectra of solids and finely powdered crystals. The usefulness of the pulsed optoacoustic technique to nonlinear spectroscopy has been demonstrated in the following studies: (a) quantitative two-photon absorption spectroscopy of the weak two-photon ($^1B_{2u} \leftarrow {}^1A_{1g}$) transition in benzene; and (b) optoacoustic Raman-gain spectra for a variety of liquids where an ability to measure Raman gains as small as 10^{-5} cm^{-1} has been demonstrated. In addition to reviewing the above studies the authors discuss future possible applications and compare the pulsed optoacoustic spectroscopy technique with other optoacoustic absorption measurement techniques.

CONTENTS

I. INTRODUCTION

The field of optoacoustic (OA) spectroscopy of condensed matter has undergone tremendous growth in the past several years. Hordvik (1977), Robin (1976), Rosencwaig (1978), and Somoano (1978) have reviewed various aspects of the field, and Pao (1977) has edited a book on the subject. The "conventional" technique of optoacoustic spectroscopy (also called photoacoustic spectroscopy) utilizes a gas-phase microphone, which senses the heating and cooling of a gas layer in thermal contact with the sample of condensed matter being irradiated by a chopped light beam. Such a technique was first used by A. G. Bell and others and has been revived recently by Harshbarger and Robin (1973) and Rosencwaig (1973). This recent work is an extension of the earlier gas-phase optoacoustic spectroscopy work (e.g., Kreuzer, 1971). Analytical studies of the signal dependence on the chopping frequency, absorption coefficient, and thermal properties have been carried out, for example, by Rosencwaig and Gersho (1976), Aamodt and co-workers (1977, 1978), and McDonald and Wetsel (1978). However, the gas-phase microphone technique for condensed samples relies on inefficient thermal diffusion into a gas, and can be viewed actually as a photothermal (Brilmyer *et al.*, 1977) technique and not a photoacoustic one, since the acoustic signal generated in the sample plays only a minor role. Thus this technique has low sensitivity (Hordvik and Schlossberg, 1977; Farrow *et al.*, 1978; McQueen, 1979), and is often only useful for absorption typically exceeding 1%. Some of the disadvantages of the inefficient coupling are partially overcome by the availability of high-efficiency gas-phase microphones. Several authors (Hordvik and Schlossberg, 1977; Farrow *et al.*, 1978) have recognized the inefficiency of the "conventional" photoacoustic technique,

and they show that improvements in sensitivity are possible with the use of piezoelectric transducers in contact with solid samples (Hordvik and Schlossberg, 1977) or liquid samples (Farrow *et al.*, 1978), but these authors still use light beams chopped at low audio frequencies.

We have recently demonstrated a highly sensitive pulsed OA spectroscopy technique (Patel and Tam, 1979a), involving the use of pulsed lasers, a piezoelectric transducer in direct contact with the liquid sample, and gated detection. This technique is truly optoacoustic in character (Hordvik, *et al.*, 1977; Farrow *et al.*, 1978) because the original acoustic pulse generated in the condensed sample is directly detected by a piezoelectric transducer. We note that many authors (Bonch-Bruevich *et al.*, 1975; Burt, 1979; Callis, 1976; Emmony *et al.*, 1976; Farrow *et al.*, 1978; Von Gutfeld and Budd, 1979; Hordvik and Schlossberg, 1977; Kohanzadeh *et al.*, 1975; Lahmann and Ludewig, 1977; Oda *et al.*, 1978; Razumova and Starobogatov, 1977; Rentzepis and Pao, 1966; Sigrist and Kneubühl, 1978; Sladky *et al.*, 1977; White, 1963) have used piezoelectric elements in contact with liquids or solids for optoacoustic detection, and the advantage of good acoustic impedance matching is generally recognized. However, our work appears to be the first to demonstrate the extremely high sensitivity of the technique for detecting weak absorptions in liquids or solids. We further note that Bonch-Bruevich *et al.* (1977) have used an optoacoustic detection scheme similar to ours, but their achieved sensitivity is at least a factor of 10^3 lower than ours.

We have applied our optoacoustic technique to several problems in linear and nonlinear optical spectroscopy. For linear spectroscopy, we have carried out (1) the first unambiguous determinations of visible absorption spectra of liquid H_2O and D_2O (Patel and Tam, 1979d; Tam and Patel, 1979b), (2) a systematic study of the absorption profiles of high vibrational overtones in benzene (Patel and Tam, 1979b; Patel et al., 1979d), and (3) studies of the absorption spectra of micron-thick liquid films (Patel and Tam, 1980) and powder films (Tam and Patel, 1979c). We show that, at present, absorption coefficients ~10^{-6} to 10^{-7} cm^{-1} can be measured. In the area of nonlinear spectroscopy, we have reported (1) the first two-photon absorption spectroscopy and cross-section measurements in liquids by optoacoustic detection (Tam and Patel, 1979a), and (2) the first Raman-gain spectroscopy of liquids (Patel and Tam, 1979c) using the pulsed optoacoustic spectroscopy technique.

The high sensitivity possible from this pulsed optoacoustic technique points to numerous further applications. In view of the wide usefulness of the technique, the present article will cover the following topics:

1. The process of pulsed acoustic generation;
2. The construction of the piezoelectric transducer, OA cell, and preamplifier;
3. Experimental results using pulsed optoacoustic spectroscopy;
4. Experimental results using other optoacoustic methods; and
5. Future applications of the technique.

Recent literature on OA studies of condensed matter is given in the reference list. We have made an effort to make the list representative of the current interest in OA studies of condensed matter; however, rapid expansion in the field of optoacoustic spectroscopy makes the omission from our list of some new contributions unavoidable.

II. THEORY

A. OA signal generation

Numerous authors have treated the problem of acoustic generation in a liquid (or in a solid) arising from the absorption of a light beam whose intensity varies with time. Most authors were interested in the case of surface heating by a pulsed laser (Askaryan *et al.*, 1963; Bell and Landt, 1967; Bushanam and Barnes, 1975; Emmony *et al.*, 1976; Gordienko *et al.*, 1978; Gournay, 1966; Von Gutfeld and Budd, 1979; Sigrist and Kneubühl, 1978; Teslenko, 1977; White, 1963), i.e., a case where most of the pulsed energy is absorbed in a thin surface layer. Other authors (Kohanzadeh *et al.*, 1975; Rosencwaig, 1978) have treated the case of the steady-state solution for a sinusoidally modulated light beam, so that all time-varying quantities have the $\exp(i\omega t)$ form. However, we are primarily interested in the case when the time-dependent signal is due to a pulsed excitation, with low optical absorption (i.e., a sample that is highly transparent to the light). This case has been considered by a few authors (Kasoev and Lyamshev, 1977; Naugol'nykh, 1977; Tam and Patel, 1979b) with varying degrees of mathematical rigor. It is interesting to note that in each of the three different cases mentioned above (surface absorption of a pulsed laser, steady-state solution for a sinusoidally modulated light beam, or weak bulk absorption of a pulsed laser) the solution is characterized by the following intuitively appealing form:

$$\frac{p_0}{E_0} = \text{const}\,\frac{\beta v_a}{C_p}\,\alpha\,, \tag{1}$$

where p_0 is the acoustic pressure amplitude developed, E_0 is the laser energy in a pulse or in a cycle, β is the thermal expansion coefficient, C_p is the specific heat at constant pressure, v_a is acoustic velocity, and α is the optical absorption coefficient of the medium. In the following we shall consider in more detail the case of weak bulk absorption of a pulsed laser beam.

We consider a thin cylinder of a liquid, illustrated in Fig. 1 (or solid if we consider only longitudinal waves), of length l and optical absorption coefficient α, irradiated by a laser pulse of duration $\tau_p = 2\tau$ and pulse energy E_0. We are primarily interested in the case of weak absorption, i.e., $\alpha l \ll 1$, so that the absorbed energy $E_0 \alpha l$ is distributed uniformly along the length l. Note that the case of large α (i.e., surface absorption) has been treated by several authors (Askaryan *et al.*, 1963; Bell and Landt, 1967; Bonch-Bruevich *et al.*, 1975; Bushanam and Barnes, 1975; Emmony *et al.*, 1976; Gournay, 1966; Sigrist and Kneubühl, 1978; and Teslenko, 1977), and results in *spherical* acoustic

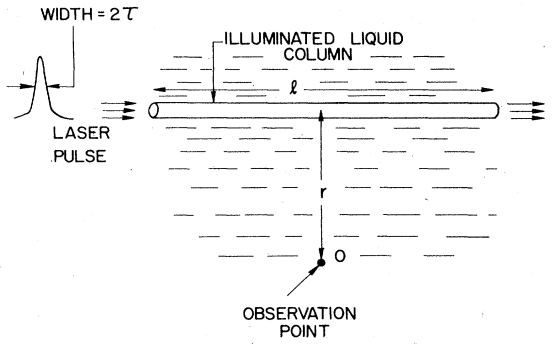

FIG. 1. Theoretical calculation of the pulsed OA effect. There is full cylindrical symmetry in the weak absorption limit for a long thin liquid column irradiated.

waves originating from the point of incidence on the surface. In our case, the weak absorption results in a *cylindrical* wave produced by the thin cylindrical volume. Here we examine the acoustic pressure $p(r, t)$ at an observation point as a function of the perpendicular distance r and time t. There is no dependence on other spatial variables besides r, since the acoustic source is assumed to be a long thin cylinder.

1. Phenomenological description of OA signal generation

The generation of an optoacoustic signal relies on the conversion of the absorbed optical radiation into heat through nonradiative relaxation processes. Rigorous derivation of the acoustic pulse generation following the absorption of a pulsed beam of optical radiation is given in the next section. Here we shall go through a phenomenological description which contains most of the physics underlying optoacoustic signal generation. The key parameter is the rapid conversion of the absorbed energy into heat by nonradiative relaxation processes. Figure 1 shows schematically a laser beam of radius R traversing a cell containing a liquid and a piezoelectric transducer placed within. The laser illumination is provided by a flash-lamp-pumped dye laser producing pulses of duration τ_p and a repetition rate of f. For the purposes of the present discussion, we assume that the laser pulse length is much longer than the nonradiative relaxation time τ_{NR}, and the time τ_a for an acoustic pulse to travel across the laser-illuminated region in the liquid, i.e.,

$$\tau_p \gg \tau_{NR}, \tag{2}$$

$$\tau_p >> \frac{2R}{v_a} \equiv \tau_a, \tag{3}$$

where v_a is the acoustic velocity in the medium. Further, we assume that the laser pulse is much longer than the response time of the piezoelectric transducer, τ_{pzt}, i.e.,

$$\tau_p \gg \tau_{pzt}, \tag{4}$$

Under these situations, achievable when using a flash-lamp-pumped dye laser, with an input pulse energy of E_0 per pulse, the energy absorbed by the medium having an absorption coefficient of α and length l is given by

$$E_{abs} = E_0(1 - e^{-\alpha l}). \tag{5}$$

For $\alpha l << 1$, a situation which we want to explore,

$$E_{abs} \approx E_0 \alpha l. \tag{6}$$

Since we are assuming that nonradiative relaxation predominates in the medium, the thermal energy E_{th} is given by

$$E_{th} = E_{abs} = E_0 \alpha l. \tag{7}$$

Knowing the specific heat at constant pressure C_p, we can evaluate the rise in temperature ΔT of the illuminated volume (neglecting thermal conduction) from

$$E_{th} = C_p V \Delta T \rho, \tag{8}$$

where V is the illuminated volume and ρ is the density of the condensed material. With

$$V = \pi R^2 l \tag{9}$$

we obtain

$$\Delta T = \frac{E_0 \alpha}{\pi R^2 C_p \rho}. \tag{10}$$

Now if we assume adiabatic, isobaric expansion, we can calculate the new volume of the illuminated region. With ΔR being the increase in the radius of the illuminated volume,

$$\pi R^2 l - \pi(R + \Delta R)^2 l = \beta V \Delta T, \tag{11}$$

where β is the volumetric expansion coefficient. By manipulation of Eq. (10), we obtain for $\Delta R << R$

$$\Delta R \approx \tfrac{1}{2} R \beta \Delta T. \tag{12}$$

Inserting ΔT from Eq. (10),

$$\Delta R = \frac{E_0 \alpha \beta}{2\pi R C_p \rho}. \tag{13}$$

This expansion creates a pressure wave which travels radially outwards from the illuminated cylinder at sound velocity. The change in pressure p created at a point is related to the frequency of the sound wave f_a and the displacement Δx through

$$p = 2\pi f_a v_a \Delta x \rho. \tag{14}$$

But Δx is proportional to ΔR evaluated in Eq. (12). Thus we have $\Delta x = \text{const} \times \Delta R$, and

$$p = \text{const} \frac{f_a}{R} \frac{\beta v_a}{C_p} E_0 \alpha. \tag{15}$$

For a fixed geometry of laser illumination and laser properties, f_a and R can be lumped into the constant. Thus we have

$$p = \text{const} \frac{\beta v_a}{C_p} E_0 \alpha. \tag{16}$$

The condition described in Eq. (3) is just satisfied for $R \approx 1$ mm, $v_a \approx 2 \times 10^5$ cm sec^{-1}, and $\tau_p \approx 1$–2 μsec for a flash-lamp-pumped dye laser.

When the illuminated cylinder is "thick" compared to the acoustic pulse propagation distance during the excitation pulse, i.e.,

$$\tau_a \gg \tau_p, \tag{17}$$

we can show (Nelson and Patel, 1980) that the transient pressure change caused by absorption of the pulse optical radiation is given by

$$p = \text{const}\,\frac{\beta v_a^2}{C_p} E_0 \alpha \tag{18}$$

when use is made of sufficiently fast transducers. Thus some care has to be exercised in using the functional dependence described in Eq. (16) or Eq. (18) for comparing optoacoustic signals from different experiments.

Since the electrical signal output from the piezoelectric transducer is given by

$$V_{oa} = \text{const} \times p \tag{19}$$

we obtain

$$V_{oa} = K' \frac{\beta v_a}{C_p} E_0 \alpha \tag{20}$$

where K' is a constant that includes the geometrical parameters as well as the response properties of the piezoelectric transducer. Now we see that the normalized optoacoustic signal S is given by (for $\tau_p \gg \tau_a$)

$$S = \frac{V_{oa}}{E_0} = K' \frac{\beta v_a}{C_p} \alpha \tag{21}$$

$$= K\alpha . \tag{22}$$

Thus a measurement of the normalized optoacoustic signal for a given substance gives direct information regarding the absorption coefficient α. Notice that while the phenomenological description obtained in Eq. (21) contains most of the important parameters necessary for the practical use of optoacoustic spectroscopy for quantitative measurements of small absorption coefficients in condensed matter, it does not provide any information regarding the shape of the optoacoustic output pulse. Detailed derivation (next section) of the acoustic pulse generation shows that the pressure pulse contains a positive going pulse followed by a negative going pulse with a time separation between the two peaks which is approximately equal to the laser pulse duration.

2. Rigorous description of OA signal generation

The problem of sound generation by a cylindrical line source has been treated in general terms by Landau and Lifshitz (1959). Following their notation, we use $\phi(r, t)$ to denote the potential of the small-amplitude acoustic wave. The velocity V and pressure p (in excess of the unperturbed value) are derivable from the potential ϕ by

$$\mathbf{V} = \nabla\phi , \tag{23}$$

and

$$p = -\rho\partial\phi/\partial t , \tag{24}$$

where ρ is the density. Landau and Lifshitz (1959) derived in their equation (73.15) for cylindrical symmetry

$$\phi(r, t) = -\frac{v_a}{2\pi} \int_{-\infty}^{t-(r/v_a)} \frac{\dot{S}(t')dt'}{[v_a^2(t-t')^2 - r^2]^{1/2}} , \tag{25}$$

where v_a is the velocity of sound, and $S(t')$ is the time derivative of the cross-sectional area $S(t')$ of the cylindrical source at retarded time t', i.e.,

$$S(t') = \pi[R + \Delta R(t')]^2$$

$$\approx \pi R^2 + 2\pi R \Delta R(t') . \tag{26}$$

Here R is the unperturbed radius of the cylindrical source and $\Delta R(t')$ is the expansion at time t' due to the laser pulse. We shall see that $\Delta R(t')$ is always many orders of magnitude smaller than R for cases of interest, so that we are justified in retaining only the lowest-order term in Eq. (26).

Now we derive p by using Eq. (24). Since a limit of integration in Eq. (25) is t dependent, it is convenient (Landau and Lifshitz, 1959) to have a change of variable $t'' = [t - t' - (r/v_a)]$ in Eq. (4) before differentiation, and change back to t' after differentiation. Thus we first write

$$\phi(r, t) = -\frac{v_a}{2\pi} \int_{-\infty}^{0} \frac{\dot{S}\left(t - t'' - \frac{r}{v_a}\right)}{[(v_a t'' + r)^2 - r^2]^{1/2}}\, dt'' \tag{27}$$

and hence we obtain

$$p(r, t) = \frac{\rho v_a}{2\pi} \int_{-\infty}^{t-(r/v_a)} \frac{\ddot{S}(t')dt'}{[v_a^2(t-t')^2 - r^2]^{1/2}} . \tag{28}$$

Using Eq. (26), we have

$$p(r, t) = \frac{\rho v_a}{2\pi} \int_{-\infty}^{t-(r/v_a)} \frac{2\pi R \Delta\ddot{R}(t')dt'}{[v_a^2(t-t')^2 - r^2]^{1/2}} . \tag{29}$$

Equation (29) is the basic "causality expression" relating the pressure at the observation point and the time derivative of the velocity of expansion of the source at retarded times.

To proceed further, we need some simple forms for $\Delta\ddot{R}(t')$. We approximate the time dependence of the pulsed laser irradiation by a Gaussian shape centered at $t' = 0$, with width of 2τ and total energy E_0:

$$\frac{dE(t')}{dt'} = \frac{E_0}{\pi^{1/2}\tau} e^{-(t'/\tau)^2} , \tag{30}$$

where $E(t')$ is the integrated laser energy up to time t' and $E(\infty) = E_0$. We further make an adiabatic approximation (i.e., neglect heat diffusion from the cylindrical source volume during the time of the laser pulse) and simply equate the volume expansion of the source at t' with that due to the temperature rise at t' neglecting any heat diffusion:

$$\pi[(R + \Delta R(t')]^2 - \pi R^2 = \beta\alpha E(t')/(\rho C_p) , \tag{31}$$

where β is the thermal expansion coefficient, and C_p is the specific heat at constant pressure (pressure fluctuation is always very small compared to equilibrium pressure in our case). We have tacitly assumed here that the laser pulse is long compared to the acoustic transit time across the cylindrical optical beam in the liquid, so that local pressure equilibrium is maintained. We note that heat diffusion is always negligible in our case, since diffusion length λ_{diff} in a time interval τ is given by

$$\lambda_{\text{diff}} = (4\tau D)^{1/2} , \tag{32}$$

where D is the thermal diffusivity. Typically, we have $\tau \sim 10^{-6}$ sec and $D \sim 10^{-3}$ cm^2 sec^{-1} for most liquids. Thus $\lambda_{\text{diff}} \sim 10^{-4}$ cm and is much smaller than typical values for R, which are within the range of 10^{-3} to 1 cm.

Neglecting the $\Delta R^2(t')$ term in Eq. (31), we have

$$2\pi R \Delta R(t') = \beta \alpha E(t')/(\rho C_p). \tag{33}$$

Combining Eqs. (30) and (33), we have

$$2\pi R \Delta \ddot{R}(t') = \frac{\beta\alpha}{\rho C_p} \frac{E_0}{\pi^{1/2}\tau} \frac{(-2t')}{\tau^2} e^{-(t'/\tau)^2}. \tag{34}$$

Substituting Eq. (34) into Eq. (29), we have

$$p(r,t) = -\frac{v_a \beta \alpha E_0}{\pi(\pi)^{1/2} C_p \tau^3} \times \int_{-\infty}^{t-(r/v_a)} \frac{t' e^{-(t'/\tau)^2} dt'}{[v_a^2(t-t')^2 - r^2]^{1/2}}. \tag{35}$$

We may call Eq. (35) the pulsed optoacoustic equation, relating the transient acoustic pressure p at the observation point to the retarded time development of the laser pulse. It has the form indicated in Eq. (1), with the "const" containing v_a, τ, and an r-dependent retarded time integral. Approximate expressions similar to Eq. (35) have also been given by other authors, e.g., Bunkin and Komissarov (1973), Lyamshev and Naugol'nykh (1976), Naugol'nykh (1977), and Westervelt and Larson (1973).

The pulsed optoacoustic signal generation described in Eq. (35) can be integrated numerically, and the predicted time dependence is yet to be compared with observations in future experiments. Simplification of Eq. (35) is possible for sufficiently large r, so that the integrand in Eq. (35) is most important when $t - t' \sim r/v_a$. Hence we can make the following approximation:

$$v_a^2(t-t')^2 - r^2 \approx 2r[v_a(t-t') - r], \tag{36}$$

and Eq. (35) becomes

$$p(r,t) = -\frac{v_a \beta \alpha E_0}{\pi(2\pi r)^{1/2} C_p \tau^3} \times \int_{-\infty}^{t-(r/v_a)} \frac{t' e^{-(t'/\tau)^2} dt'}{[v_a(t-t') - r]^{1/2}}. \tag{37}$$

From Eq. (34) we see that the source term $\Delta\ddot{R}(t')$ has the largest amplitude at $t' = \pm 0.7\tau$, and vanishes rapidly at large $|t'|$. Thus we would also expect $p(r,t)$ to be of largest magnitude at $t_\pm \approx r/v_a \pm 0.7\tau$. Approximate evaluation of the integral in Eq. (36) shows that

$$p(r,t_\pm) \approx \pm \frac{\beta \alpha E_0}{\pi C_p \tau^2} \left(\frac{v_a \tau}{2\pi r}\right)^{1/2} \equiv \pm P_0(r). \tag{38}$$

Several interesting observations are possible with the pressure amplitudes predicted in Eq. (38). First, we note that the compression pulse at time t_- is followed by a rarefaction pulse (of nearly equal magnitude) at time t_+, with the time interval between the compression and rarefaction being approximately the laser pulse width. This prediction has been noted by several authors (Bunkin and Komissarov, 1973; Lyamshev and Naugol'nykh, 1976; Naugol'nykh, 1977). Secondly, the pressure amplitude $p(r,t)$ decreases with distance as $r^{-1/2}$; this is in accordance with the conservation of energy in cylindrical symmetry, as noted by Landau and Lifshitz (1959) [Eq. (70.8)]. Thirdly, we can estimate from Eq. (38) maximum pressure amplitudes that can be expected for our typical experimental conditions of $\beta \sim 10^{-4}$ K^{-1}, $\alpha \sim 10^{-3}$ cm^{-1} (or less), $E_0 \sim 10^{-3}$ J, $C_p \sim 1$ J gm^{-1} K^{-1}, $\tau \sim 10^{-6}$ sec, $v_a \sim 10^5$ cm sec^{-1}, $r \sim 1$ cm. With these values substituted in Eq. (38), we estimate

$$P_0 \sim 10 \text{ dyn cm}^{-2} \sim 10^{-5} \text{ atm}. \tag{39}$$

Thus pressure fluctuations are always much less than the equilibrium pressure (1 atm in our experiments so far). Furthermore, we can estimate the maximum expansion ΔR from Eq. (33) if we put $R \sim 10^{-2}$ cm and $\rho \sim 1$ gm cm^{-3}. We thus have

$$\Delta R \sim 10^{-9} \text{ cm}. \tag{40}$$

This indicates that we are always dealing with small-amplitude waves.

In the above derivation, we have assumed that the irradiated region is a thin cylinder, i.e., $R \ll r$. If this is not true, we may subdivide the irradiated cylinder of radius R into many thin cylinders, each being an acoustic source. The pressure at the observation point O will be the algebraic sum of pressures produced by these line sources. If $R \ll v_a\tau$, then the double acoustic pulses from all the line sources are in phase, and we should still have a compression and rarefaction pulse at the observation point separated approximately by τ. However, if $R \gg v_a\tau$, then the double pulses from various line sources are out of phase and cancellation occurs, with the results that the compression and rarefaction pulses at the observation point will now be separated by R/v_a, the "transit time" across the source. In any case, the acoustic amplitude is still of the general form given by Eq. (1).

Naugol'nykh (1977) has derived approximate solutions for the acoustic pressure pulse generated in a liquid subsequent to the absorption of an optical pulse energy and the release of the absorbed energy through nonradiative processes. His expressions are as follows.

a. For a thin illuminated cylinder, i.e., $R \ll v_a\tau_p$.

$$p \approx \left(\frac{1}{\pi R r \tau_p}\right)\left(\frac{\beta v_a}{C_p}\right) E_0 \alpha. \tag{41}$$

b. For a thick illuminated cylinder, i.e., $R \gg v_a\tau_p$.

$$p \approx \left(\frac{1}{r\pi R^2}\right)\left(\frac{\beta v_a^2}{C_p}\right) E_0 \alpha. \tag{42}$$

The distinction between the two cases depends upon the relative dimensions of the radius of the illuminated region [see Fig. 1 and also Eqs. (16) and (18)] and the spatial scale of the acoustical pulse. We have assumed here that the time duration of the acoustical pulse is the same as that of the optical excitation pulse, a case which is applicable when the nonradiative decay of the absorbed optical energy is much faster than the duration of the optical pulse. The case (a) for $R \ll v_a\tau_p$

(thin cylinder geometry) is applicable to the long-excitation-pulse, focused radiation experiments such as the nonlinear optoacoustic experiments described later in this paper where $R \lesssim 0.01$ cm and $v_a \tau_p$ for microsecond excitation is ≈ 0.2 cm. For the linear optoacoustic absorption studies where the incident laser radiation is not focused we are just out of the thin cylinder case (a), $R \ll v_a \tau_p$ since $R \approx 2$ mm. With the use of dye laser pulses of shorter duration, such as those obtained from Q-switched doubled Nd:YAG laser-pumped dye lasers, we would always be in the thick cylinder regime (b), i.e., $R \gg v_a \tau_p$. It is then necessary to use the appropriate scaling relations involving β, v_a, ρ, and C_p for transferring the absolute calibration from one liquid to another as we see in what follows. Lyamshev and Naugol'nykh (1976) have also derived similar expressions for spherical volumes but these do not correspond to any of the experimental results reported here and thus they will not be discussed here.

Gorodetskii *et al.*, (1978) have also carried out detailed analysis of sound generation by absorption of optical pulses in liquids. Their general results do not differ from those of Naugol'nykh (1977) or those derived above. Further, they have measured the acoustic pulse amplitude (using a piezoelectric transducer) produced in water through the absorption of a 15 nsec Nd:YAG laser (1.06 μm) pulse in water, which has an absorption coefficient of ~0.14 cm^{-1} at $\lambda = 1.06$ μm—a number which is very large compared to what optoacoustic spectroscopy is ideally suited for measuring. They also have verified (over a rather limited range of 7 to 17 °C) the variation of the optoacoustic signal with β of water whose temperature dependence is known. Further, for even larger absorption coefficients at 1.06 μm, obtained by the addition of copper sulfate to water when the optical absorption occurs over small distance, they have studied the angular distribution of the acoustic signal amplitude.

B. Acoustic pulse arrival time

A further point not clearly seen from Eqs. (16) and (18), but apparent from Eq. (38), is the time delay between the laser pulse and the arrival of the pressure pulse at the piezoelectric transducer placed at a distance r from the laser-illuminated cylinder as shown in Fig. 1. The time delay τ_d is given by

$$\tau_d = \frac{r}{v_a} . \tag{43}$$

This time delay is a crucial parameter in implementation of the optoacoustic techniques for absorption spectra measurements, in that the delay allows the use of proper time gating of the output signal, using a boxcar averager to discriminate against undesirable transients.

C. Calibration of OA spectroscopy

Equations (16), (18), and (19) are, of course, the bases of pulsed optoacoustic spectroscopy: V_{oa} is measured by a piezoelectric transducer in direct contact with the sample, and E_0 is measured by an optical detector (generally a pyroelectric detector which has wavelength-independent sensitivity); the ratio V_{oa}/E_0, defined as the normalized optoacoustic signal $S(\nu)$, is obtained as a function of the laser frequency ν. By Eq. (1),

$$S(\nu) = K\alpha(\nu) , \tag{44}$$

with the constant of proportionality K dependent on sensitivities of the detectors, on the properties of the sample (e.g., β, C_p, v_a) and on geometry and laser pulse shape.

In principle, the proportionality constant K can be estimated theoretically by evaluating Eq. (38) together with knowing the efficiencies of the detectors. In practice, K must be measured experimentally for a given liquid by comparing the normalized OA signals S and S' for the pure liquid and the liquid doped with a dye. Several conditions must be satisfied for the dye to be useful:

(1) It should be strongly absorbent in the wavelength of interest so that only a very dilute doping is needed to cause significant increase in optical absorption (dilute doping implies that the thermoelastic properties of the solution and the pure liquids are the same);

(2) No significant fluorescence of the dye should be produced;

(3) No photochemical reaction of the doped solution should occur;

(4) The dye should be stable in the OA cell (for example, it should not be absorbed by the cell wall either through chemical reaction or adsorption).

With these conditions satisfied, we can apply Eq. (44) to the cases of the pure liquid and the doped liquid:

$$S = K\alpha_0 \tag{45}$$

and

$$S' = K(\alpha_0 + \alpha_1) , \tag{46}$$

where α_0 is the absorption coefficient of the pure liquid at the wavelength investigated, and α_1 is the additional absorption at the same wavelength due to the dye. We can use a dual-beam spectrophotometer, and two cuvettes containing the pure liquid and the doped liquid, to determine α_1 independently. Thus we can solve K as

$$K = (S' - S)/\alpha_1 . \tag{47}$$

Having obtained K for a given experimental situation (at one wavelength), we can proceed and obtain $\alpha(\nu)$ from the measured $S(\nu)$ using Eq. (44).

D. Sensitivity

The sensitivity of the optoacoustic technique described above was determined by measuring the weak sixth harmonic of vibrational absorption (Patel and Tam, 1979a; Tam, Patel, and Kerl, 1979) in C_6H_6 (see Sec. V.A.2 for spectroscopy) with increasing dilution in CCl_4, which has very small absorption in the wavelength region of interest. Without going into detail, we have shown (Tam, Patel, and Kerl, 1979) that absorption coefficients as small as $\sim 10^{-6}$–10^{-7} cm^{-1} can be measured (with a signal-to-noise ratio of 1, input pulse of energy of ~1 mJ/pulse, pulse repetition frequency of 10 sec^{-1}, and integration

time of 1 sec).

The factors affecting and limiting the sensitivity of the measurement technique include (a) optical absorption signals from windows, (b) light scattering in the bulk of the liquid, and (c) electrostriction. The signals arising from the first two can be minimized by (1) choice of low-loss windows, (2) reduction of scattering impurities in the liquid, (3) appropriate time gating of the acoustic signals observed from the piezoelectric transducer. The time gating is very important, since scattered light travels at the velocity of light in the medium, $v_c = c/n$, where n is the refractive index of the material, while the acoustic signal generated in the bulk will travel at the acoustic velocity v_a in the medium. Thus the signals arising from the scattered light being absorbed by the transducer will occur essentially promptly after the laser pulse, while the bulk acoustic signal is delayed by τ_d defined in Eq. (43). For the case of acoustic signals from optical absorption by the windows, the acoustic pulse arrives after that originating from the bulk. The acoustic pulse generated due to electrostriction processes in the laser-irradiated region is, however, of similar form to that arising from the bulk absorption, and hence there is no reasonable way in which the two can be distinguished. The electrostriction signal pulse is estimated (Brueck *et al.* 1980) to be of comparable size to that arising from optical absorption for $\alpha \approx 10^{-6}$ cm^{-1}. Brueck *et al.* studies, however, were biased to show the superiority of the photorefractive technique over the pulsed optoacoustic technique. This can be clearly seen from their use of short laser pulse duration of ~70 nsec (giving rise to high peak powers and the attendant high optical frequency electric fields which determine the electrostriction effects), and tight focusing of the incident laser beam (200 μm diameter), even for linear absorption studies. The latter gives rise to high optical intensities and correspondingly high electric fields to accentuate the effects of electrostriction. It can be shown that the absorption coefficient at which the optoacoustic signal and the acoustic signal due to the electrostrictive effect become *equal* is inversely proportional to the diameter of the laser spot size. Thus, for typical linear optoacoustic spectroscopy studies where the laser spot size is rarely smaller than ~3 mm, the acoustic signal arising from the electrostrictive effect would equal that arising from optoacoustic effect for optical absorption coefficient $\alpha_1 \approx 6\times10^{-8}$ cm^{-1} even keeping the laser pulse length fixed. Further, if we extrapolate to the case of long laser pulse lengths of 1 μsec used in most of the present studies, the optical absorption coefficient α_1 becomes $\sim 4\times10^{-9}$ cm^{-1}, a value which is much smaller than that estimated by Brueck *et al.* Finally, there is no (or only very weak) dependence of the electrostriction pulse on laser wavelength. Hence, even the 4×10^{-9} cm^{-1} level does not represent a limitation on the smallest absorption coefficient that can be measured using the optoacoustic spectroscopy if the material being studied has a wavelength dependent absorption. Subtraction of background signal (constant) as large as a factor of 10 to 100 times that corresponding to a well-defined peak can easily be subtracted electronically.

Bebchuk *et al.* (1978) were one of the first to investigate the interference effects of electrostriction in optoacoustic spectroscopy using pulsed lasers and immersed (or attached) transducers. However, their observations that an optical absorption coefficient of ~3 cm^{-1} gave optoacoustic signals only a factor of ten larger than those arising from electrostriction surely is in error, since our experimental spectroscopic data show that electrostriction plays no role in the optoacoustic signal for absorption coefficients as small as 10^{-7} cm^{-1}.

III. APPARATUS

In this section we present a detailed description of our experimental apparatus for pulsed OA spectroscopy of condensed matter. Most of our discussions are concerned with liquids. The case of solids (mainly powders) is discussed in Sec. III.D.

A. Transducer

In recent years, several authors have realized that the photoacoustic spectroscopy scheme (Harshbarger and Robin, 1973; Rosencwaig, 1973; Rosencwaig and Gersho, 1976; Rosencwaig, 1977; Rosencwaig, 1978; Rosencwaig *et al.*, 1979) first used by Harshbarger and Robin (1973), and by Rosencwaig (1973), utilizing gas-phase microphones, is quite insensitive for OA studies of condensed matter. Thus the technique of piezoelectric detection of the OA signal has been used by Lahmann *et al.* (1977), Bonch-Bruevich *et al.* (1977), Sladky *et al.* (1977), Farrow *et al.* (1978), Burt (1979), and others. The reason is that acoustic impedance matching is very good for piezoelectric detectors directly coupled to solids, and acoustic transmission exceeding 50% from from the solid to the detector is generally possible. For liquids, the transmission generally exceeds 10%. This is in sharp contrast to the transmission across an interface between condensed matter and gas, where the transmission is typically ~10^{-5}. (Some of the coupling inefficiency is made up by the very high sensitivities of commercially available gas microphones.)

Various piezoelectric transducers have been used. A geometry that seems to be most popular is a piezoelectric cylinder that actually encloses the liquids (Lahmann *et al.*, 1977; Sladky *et al.*, 1977; Farrow, 1978; Oda *et al.*, 1978; Burt, 1979). However, we found that it is easier and more reliable to use a home-made transducer with a flat face that protrudes into the liquid being studied. The construction and the advantages of such a transducer are discussed below.

Figure 2 shows the construction of our piezoelectric transducer (Tam and Patel, 1979b). The heart of the transducer is a lead zirconate-lead titanate (PZT) cylinder that is poled axially and silvered on both ends. The cylinder, of diameter 4 mm and height 4 mm, is purchased from Transducer Products of Connecticut (material LTZ-2). This material is commonly used in hydrophones because of its high sensitivity, high long-term stability, and resistivity at elevated temperatures. It is nearly identical to the more commonly known material PZT-5A produced by Vernitron of Ohio. The height of the cylinder is chosen to provide a rise time

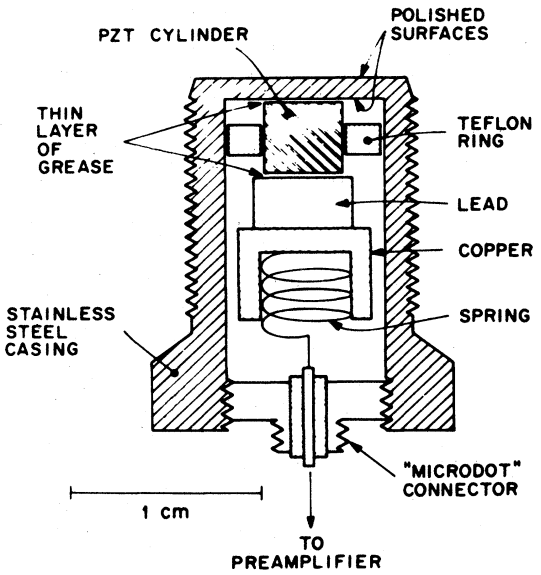

FIG. 2. Cross section of the homemade piezoelectric transducer utilizing a lead-zirconate-titanate cylinder (LTZ-2 or PZT-5A).

~1 μsec, which is fast enough to detect the OA ultrasonic signal generated in our experiments.

The PZT cylinder is firmly mounted in a stainless steel casing, as illustrated in Fig. 2. The front diaphragm of the casing (about 1 mm in thickness) is polished on both sides. The PZT cylinder is spring-loaded against the diaphragm, with a thin layer of silicone grease applied between them to ensure good acoustic coupling. The backing plate of the PZT cylinder is a lead disc soldered to a copper disc. The use of lead (which has high ultrasonic attenuation) leads to reduced acoustic reflection back into the PZT transducer, thus reducing "ringing" effects. A thin layer of grease is also applied between the PZT cylinder and the backing plate. The OA signal is fed through the phosphor bronze spring to the microdot connector, as shown in Fig. 2.

For our purposes, this transducer has a performance comparable to or better than that of commerical hydrophones (which are available from numerous companies, like Celesco of California or KSP Industries of Virginia). However, besides good sensitivities [$\sim 3\times 10^{-5}$ V/(N m^{-2})], our transducer has several important advantages over commerical hydrophones:

(a) The flat polished front face of the transducer reflects most of the stray light scattered onto it; furthermore, the large thermal mass and conductivity of the diaphragm minimize the effect of light absorption;

(b) Nucleation of microbubbles is unlikely on the polished stainless steel face of the transducer;

(c) There is less likelihood that the liquid sample being studied will be contaminated by the stainless steel transducer than by other materials (like silver, aluminum, or epoxies);

(d) The enclosing of the PZT cylinder in a metal casing minimizes electrical pickup;

(e) The acoustic impedances of stainless steel and the PZT material are nearly the same, so that acoustic loss due to the presence of the front diaphragm is small.

We note that most commercial hydrophones have a front seal made of plastics (e.g., neoprene or epoxies), and thereby lack the above advantages. Furthermore, we note that if we had used the more commonly practiced method (Farrow *et al.*, 1978; Hordvik and Schlossberg, 1977; Oda *et al.*, 1978) of directly exposing the PZT cylinder to the liquid instead of coupling through a stainless steel diaphragm, we would have lost the advantages accrued from points (a)–(d) above.

We have chosen the PZT material with the lowest mechanical Q for our transducer, to minimize mechanical ringing of the transducer. Our PZT material has a Q that is an order of magnitude smaller than some other PZT materials. However, a significant degree of ringing still occurs. This does not constitute a major problem for our OA studies so far, but if the true time development of the OA signal is to be studied, then the degree of transducer ringing needs to be further reduced. In these cases, the use of suitable piezoelectric films (Wickramasinghe *et al.*, 1978), like ZnO or polyvinylidene fluoride, may be necessary.

B. Transducer preamplifier

Since the OA signal has an amplitude usually $\lesssim 10^{-6}$ V, suitable low-noise preamplification is necessary to increase the signal amplitude sufficiently for boxcar detection. This can best be done by using a battery-powered preamplifier located near the transducer. Since substantial overall amplification must be used, the amount of electrical pickup must be minimized. As mentioned earlier, the purpose of mounting the PZT cylinder inside the stainless steel casing is to minimize pickup. Various preamplifiers have been used by us, and we find commercial preamplifiers like Ithaco Model 143F to be satisfactory. However, lower noise is obtained with a homemade preamplifier with about 40 dB gain, designed by G. L. Miller and implemented by R. J. Kerl. This preamplifier is used in most of our studies, and the circuit for it is given in Fig. 3. Here $Q1$ is a low-noise junction field-effect transistor

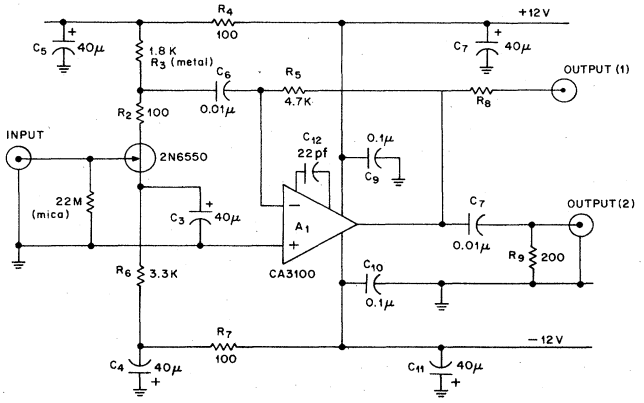

FIG. 3. Suitable preamplifier circuit (gain ~40 dB) for the transducer (modified from a circuit designed by G. L. Miller of Bell Laboratories).

(FET) (Teledyne-Crystalonics type 2N6550) having a series noise spectral density of ~1 nV $Hz^{-1/2}$, corresponding to a series noise resistance R_s of ~50 Ω. The system parallel noise resistance R_p is dominated by the equivalent loss resistance of the piezoelectric transducer employed, and is ~3.5 kΩ at 1 MHz.

The total input capacitance C_T, comprising the transducer together with the stray capacitances and the preamplifier input capacitance, is ~140 pF. This value, together with R_p and R_s, yields a noise corner time constant

$$T_c = C_T(R_p R_s)^{1/2}. \tag{48}$$

T_c in our case is evaluated to be 0.06 μsec. The preamplifier low-frequency rolloff is set by $R3C3$, while the high-frequency limit is set by $A1$ together with its (trimmed) stability capacitor $C4$. Two outputs are provided, a wideband one via $R8$ and an optional 2 μsec clipped version set by $C7R9$.

The OA signal is further amplified by an amplifier (Princeton Applied Research Model 113) before being fed to a boxcar integrator.

C. OA cell

A sketch and a photograph of our OA cell for liquids is shown in Figs. 4 and 5. The cell body is bored out of a cube of stainless steel, 2.5 cm on each side. The bore is 1.3 cm in diameter, and the surface of the bore is electropolished. High polish results in good reflectivity for the scattered light, so that spurious signals due to absorption of stray light at the cell walls can be minimized. As can be seen from Fig. 4, the front surface of the transducer extends into the bore of the OA cell. A pipe attached to the side of the cell allows direct distillation of the liquid into the cell. The cell is equipped with two fused quartz windows, which are seated in stainless steel flanges as shown; teflon O-rings are used between the quartz window and the end surface of the cell. To minimize possible contamination of the liquid sample being studied, the only materials exposed to the liquid are stainless steel, quartz, or teflon. Figure 5 shows a photograph of the stainless steel optoacoustic cell.

We have chosen stainless steel as the main construction material of the OA cell. Since stray light absorbed at cell walls constitutes a possible source of large spurious signals, the choice of material needs to be examined carefully. When stray light is absorbed

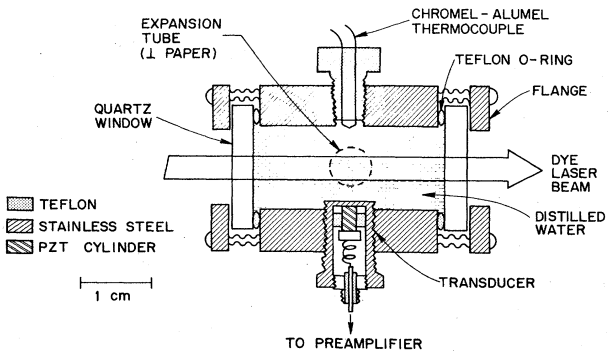

FIG. 4. Schematic drawing of stainless steel optoacoustic cell.

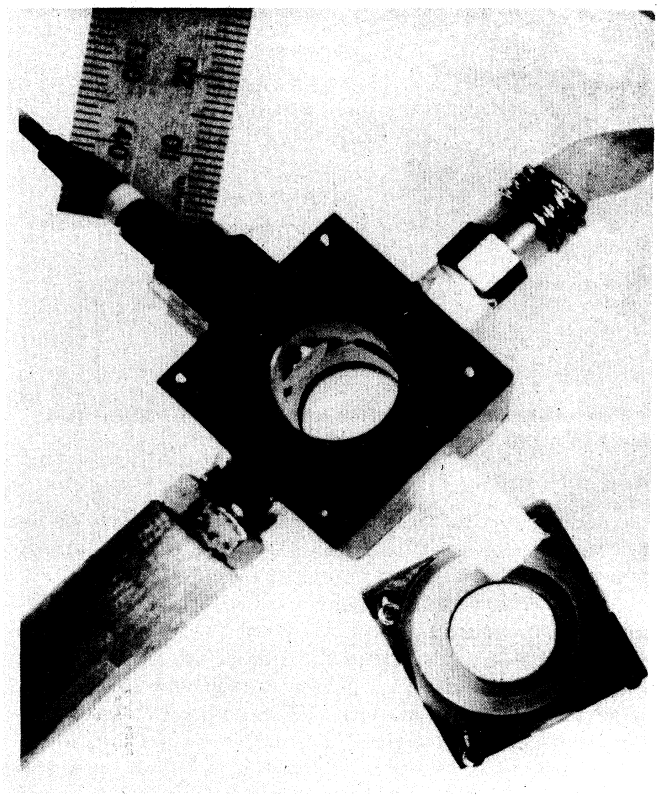

FIG. 5. Photograph of the stainless steel OA cell with a flange containing a quartz window removed. The polished transducer front diaphragm protruding into the cell can be clearly seen.

at the cell wall, the heat generated is distributed over a diffusion depth λ_{diff} as given by Eq. (32). This is assuming that λ_{diff} (~10^{-3} cm for our cases) is much greater than the optical absorption length (~10^{-5} cm for metals). The heat distributed over the depth λ_{diff} causes a temperature rise ΔT_{wall} given by

$$\Delta T_{wall} = \text{const}/(\lambda_{diff}\rho C_p) \tag{49}$$

where ρ and C_p are the density and specific heat of the metal. The "const" in Eq. (49) contains surface optical-absorption and reflection factors. We see from Eq. (49) that construction material for the OA cell should have small surface optical absorption, large thermal diffusion length, high density, and specific heat. In this respect, silver or aluminum are a better choice than stainless steel; the factor $1/(\lambda_{diff}\rho C_p)$ is smaller in silver or aluminum than in stainless steel by roughly a factor of 2. However, the high degree of chemical reactivity of silver or aluminum makes the choice of stainless steel a reasonable compromise.

D. Arrangement for films or powders

We have recently developed (Patel and Tam, 1980; Tam and Patel, 1979c) a modified form of the OA cell for spectral analysis of thin liquid films or for films of powders. This modified arrangement is shown in Fig. 6. The film sample to be studied (typically several microns in thickness) is clamped between fused quartz plates, and the OA signal generated in the liquid or solid film is launched as acoustic waves (both trans-

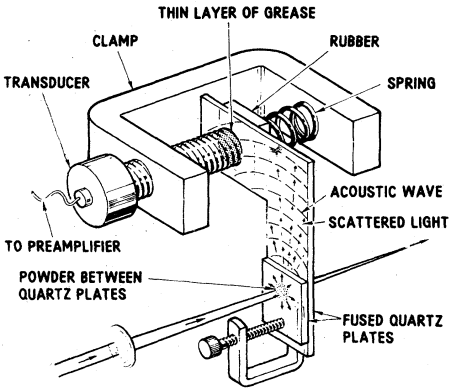

FIG. 6. Suitable OA "cell" for films, powders, or any thin layer of highly light-scattering material.

verse and longitudinal, and possibly also surface acoustic waves) into the substrate. Quartz has a very small absorption coefficient α_{us} for ultrasonic waves ($\alpha_{us} \sim 10^{-3}$ cm^{-1} at a frequency of 1 MHz), and so little absorption occurs between the point of generation of the OA signal (i.e., irradiated position of the film) and the point of detection (i.e., the transducer). Although quartz is an excellent substrate material for the present purpose of OA studies of films, common microscope slides are found to be much less useful, resulting in an OA signal an order of magnitude smaller than in the quartz case. The reasons for this big difference are unclear.

The apparatus shown in Fig. 6 is also found to be ideally suited (Tam and Patel, 1979c) for OA spectroscopy of powders, which may be cooled to low temperature by refrigerating the part of the substrate containing the powder. We first make a suspension of the powder in a transparent viscous carrier liquid (e.g., ethylene glycol). Then we place a small drop of the suspension on a quartz substrate, and cover it with a quartz cover plate. Intense light scattering is observed, and this would generally constitute a major source of spurious signals in an OA study. However, the disastrous effects of intense light scattering are nearly eliminated in our experimental arrangement, shown in Fig. 6, for the following reasons: (a) the quartz plates sandwiching the powder film (approximately several microns thick) are approximately 1 mm in thickness; this thin sandwich geometry allows most of the scattered light to escape and a very small amount of the scattered light is trapped in the substrate; (b) as can be seen in Fig. 6, the substrate has a right-angle bend, and hence most of the light trapped in the substrate cannot reach the transducer. Further reduction in the amount of scattered light reaching the transducer can be achieved by having more right-angle bends in the substrate. On the other hand, acoustic waves launched into the substrate can readily diffract around the bends and reach the transducer; and (c) the effect of the small amount of light that actually reaches the transducer indirectly can be minimized by a time gating technique. This is possible because of the much faster speed of light than the speed of sound, and so the spurious signals due to light scattering onto the transducer occur immediately, while the desired OA signal begins only after an acoustic propagation time. The time-gating technique is discussed further in Sec. IV.

The geometry of the substrate (a right-angle bend, of width ~1 cm and length of each arm ~10 cm) has a waveguiding effect for the OA waves, and very efficient detection of the OA signal can be achieved. The detection is done with a PZT transducer identical to that used for liquids (Fig. 2). The flat polished front diaphragm of the transducer is now firmly spring-loaded against the quartz substrate at the position indicated in Fig. 6. A thin layer of silicone grease is used between the transducer and the substrate to facilitate acoustic coupling.

IV. EXPERIMENTAL PROCEDURE

The block diagram for the experimental investigation of weak absorption in liquids is shown in Fig. 7. The apparatus is very simple, yet it can presently detect absorption coefficients as small as 10^{-7} cm^{-1}. This represents an improvement in detectability by a few orders of magnitude over that previously achieved with conventional OA measurements (Harshbarger and Robin, 1973; Rosencwaig, 1973; Rosencwaig and Gersho, 1976; Rosencwaig, 1977; Rosencwaig, 1978). Further improvement in detectability is possible by using, for example, more powerful and stable laser sources, better shielding against acoustic noise and electrical pickup, and a better cell design (e.g., multipass geometry, windows farther away from the transducer, antireflection-coated windows with as small optical absorption as possible, etc.).

The light source used in our studies so far is a commercial scannable flash-lamp-pumped dye laser, producing ~1 mJ energy and 1 μsec duration pulses, at a laser bandwidth (full width at half maximum FWHM) of ~2 cm^{-1}. With the use of various dyes, we can cover the visible region from ~450 nm to ~700 nm. It is usually operated at 10 pulses/sec. The bandwidth of 2 cm^{-1} is adequate for most liquids and solids; indeed, a bandwidth ~100 cm^{-1} is frequently adequate for resolving spectral features of condensed matter,

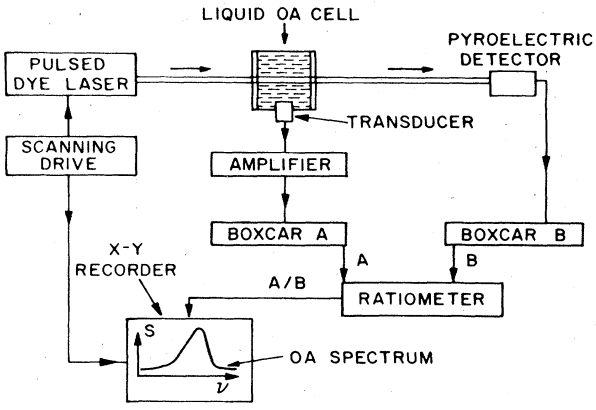

FIG. 7. Block diagram of the simple experimental arrangement needed for linear spectroscopy of liquids with the pulsed OA detection method.

and so pulsed arc light sources together with a scannable low-resolution monochromator can be used instead of the laser. However, in certain studies (e.g., investigation of rare-earth oxide powders at low temperature), resolution of 0.1 cm^{-1} or better may be needed, and narrow-band laser sources must be used.

As shown in Fig. 7, the transient OA signal is amplified and measured by a boxcar integrator A. The laser pulse energy is monitored by a pyroelectric detector, whose output signal is amplified and measured by a boxcar integrator B. The pyroelectric detector presently used is a coated lithium niobate detector (Laser Precision Model 2050S), which has a flat spectral response (flat to within ±2%) from near uv to near ir, and is sufficient for our studies so far. However, when higher accuracies are needed over an extended spectral range, better pyroelectric detection (e.g., models with multiple reflections) with improved spectral flatness will be required. The boxcar outputs A and B are fed to a ratiometer and the ratio A/B (defined as the normalized OA signal S) is obtained as the laser frequency ν is scanned. (This normalization procedure is for linear absorption; slightly different normalization procedure is needed for nonlinear absorption spectroscopy, as discussed later.) Subsequent to our initial studies where we used the ratiometer for obtaining A/B, we have replaced the ratiometer by a minicomputer which digitizes the signals A and B from the boxcars and also keeps track of dye laser frequency through an appropriate readout unit. The output, then, is the A/B value as a function of frequency, which is plotted and printed as necessary. The advantage of using the minicomputer system (a system using a relatively inexpensive microprocessor can be used instead of the minicomputer) is the increased dynamic range in the ratio determination and the digital information, which makes it easy to join up sections of $S(\nu)$ vs ν data obtained by using different dyes for different spectral regions. We have seen in Eq. (44) that $S(\nu)$ is proportional to $\alpha(\nu)$; with the proportionality constant determined by Eq. (47), an absolute absorption spectrum is obtained.

We now describe some experimental observations that support the theories of pulsed OA signal generation; in particular, we want to verify the pulsed OA Eq. (1). An OA signal detected by the piezoelectric transducer is shown in Fig. 8. The signal begins at a well-defined delay time t after the occurrence of the peak of the laser pulse. This delay time t is found to be linearly dependent on the distance d between the laser beam and the transducer surface. By moving the cell with a micrometer translation stage, d can be varied by several mm, and t is observed to change by several μsec. The dependence of the change in delay Δt on the change in distance Δd is shown in Fig. 9, where the reciprocal of the gradient is found to be $(1.32 \pm 0.04) \times 10^5$ cm sec^{-1} for the case of a benzene-filled OA cell at 20 °C. This is in excellent agreement with the established ultrasonic velocity at room temperature in benzene, being 1.326×10^5 cm sec^{-1}. Thus we are detecting a ballistically-propagating OA signal from the laser-irradiated column of liquid. Our boxcar gate (shown in Fig. 8) is set to detect the amplitude of the early part of the OA signal. This is because later parts are found to be more liable to be contaminated by spurious absorptions, e.g., at the cell windows. This is especially important when very weak absorption features of the liquid are being studied. The above technique of time gating is also very useful for the case of powdered samples, where intense light scattering occurs. Figure 10 shows an observed OA signal for fine powders of Ho_2O_3, in the experimental arrangement shown in Fig. 6. There is a very important difference between the OA signals detected when the laser is tuned on resonance or off resonance of an absorption feature of Ho_2O_3. For the off-resonance case, signals are observed almost immediately after the laser pulse, because of some residual amount of scattered light that reaches the transducer. This unwanted signal decays, with a time constant of some tens of μsec. For the on-resonance case, the same unwanted signal appears; however, after an acoustic propagation time, an extra signal appears due to the OA wave launched into the substrate by the powder. Hence by gating the OA signal at an appropriate delay (as shown in Fig. 10), the masking effect of the unwanted signal caused by light scattering can be strongly suppressed. Further improvements in rejection of scattered-light-induced signals has been accomplished by having multiple bends

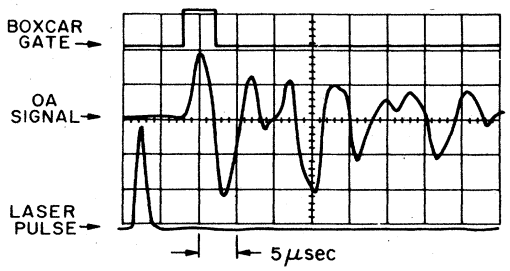

FIG. 8. Oscilloscope picture shows the laser pulse (lower trace), OA signal (middle trace), and boxcar gate for the OA detection (upper trace) for a typical liquid.

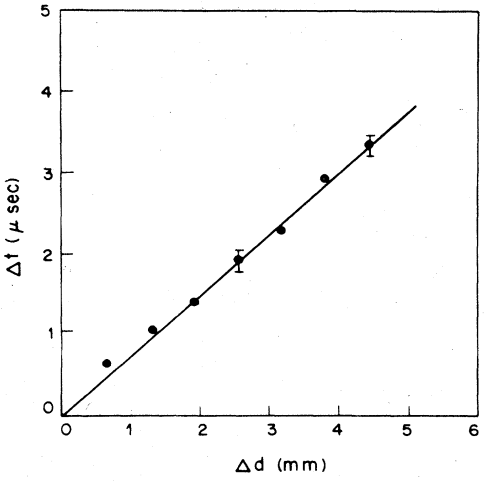

FIG. 9. Dependence of the change in delay time (Δt) on a change in the beam-transducer separation (Δd). The line through the data point corresponds to the ultrasonic velocity in the liquid.

in the quartz substrate. This is indicated in Fig. 11, where the scope pictures (A) and (B) correspond to a substrate with a single bend, and (C), (D), and (E) correspond to a substrate with multiple bends, as shown in the corresponding drawings on the right. For Fig. 11, the powder sample being examined is Ho_2O_3; the dye laser is on an absorption line at 18 735 cm^{-1} (line No. 8 in Fig. 24) for pictures (A) and (C), but for pictures (B) and (D), the dye laser is detuned away from an absorption line, i.e., the dye laser frequency is set at 18 800 cm^{-1} where there is little or no absorption by the Ho_2O_3 powder. In picture (E), the dye laser beam is blocked. In Fig. 11(A), the laser pulse is shown on the lower trace. The delay of ~25 μsec seen between the laser pulse and the onset of the optoacoustic signal is understood as the propagation time for the acoustic pulse to travel from the illuminated region to the transducer. In Fig. 11(B), the OA signal is much reduced; however, the small signal that we see arises primarily from the scattered light reaching the transducer, suggesting incomplete elimination of the scattered-light problem. Figure 11(C) shows, again, the OA signal for the on-resonance case for the new geometry. Two points should be noted. First, the start of the signal trace is delayed from the laser pulse by an additional 50 μsec. Thus the total acoustic delay is 75 μsec, which is consistent with the acoustical propagation time in the quartz substrate in which the acoustic pulse is launched from the absorption of laser light in Ho_2O_3. The second point to notice is that the amplitude of the acoustic pulse is identical with that in Fig. 11(A) for a shorter acoustic propagation distance, indicating that for the distances involved here, there is little or no acoustic absorption for the frequencies involved. Figure 11(D) shows the dramatic improvement that is obtained for the off-resonance laser radiation. Comparison of Figs. 11(B) and 11(D) indicates that the scattered-light-induced signal is now reduced by at least an additional factor of 5. That the actual reduction is more than this factor can be seen by comparing Fig. 11(D) with Fig. 11(E), which shows the signal from the transducer with the laser blocked. The lack of any significant differences between Figs. 11(D) and 11(E) is a convincing demonstration that the multiple-bend arrangement shown in Fig. 11 *completely* eliminates the scattered-light problem associated with the optoacoustic study of powder samples.

The linearity of the observed OA amplitude versus the laser pulse energy has been verified for linear absorption in various liquids (e.g., benzene, acetone, water, etc.) at various absorption levels, from absorptions coefficients larger than 10^{-3} cm^{-1} to those smaller than 10^{-5} cm^{-1}. This linearity is in accordance with Eq. (1). An example of our linearity study is shown in Fig. 12, which shows a plot of the amplitude of the OA signal measured by the transducer at various laser pulse energies, which are varied by calibrated neutral-density filters. The data of Fig. 12 correspond to liquid benzene, with the laser tuned to 18 810 cm^{-1} (peak of the seventh harmonic of the C–H stretch in benzene). Good linearity is clearly observed.

The dependence of the OA signal on the thermal expansion coefficient β, as given in Eq. (1), has also been verified experimentally. This is found to be most con-

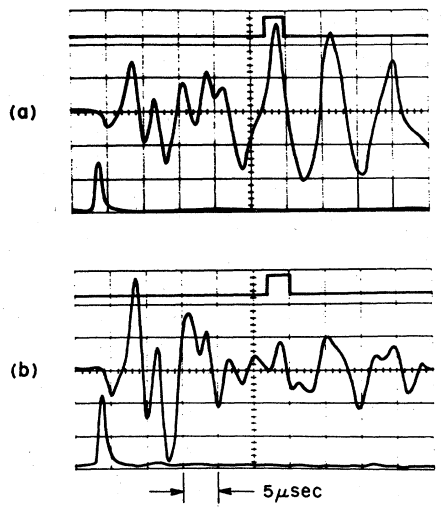

FIG. 10. Each scope picture shows the laser pulse (lower trace), transducer signal (middle trace), and gate position of boxcar *A* (upper trace). Time scale = 5 μsec cm^{-1}. Powder sample is Ho_2O_3. (a) Laser tuned to the absorption line at 18 633 cm^{-1}. (b) Laser tuned off an absorption line (laser frequency at 18 800 cm^{-1}).

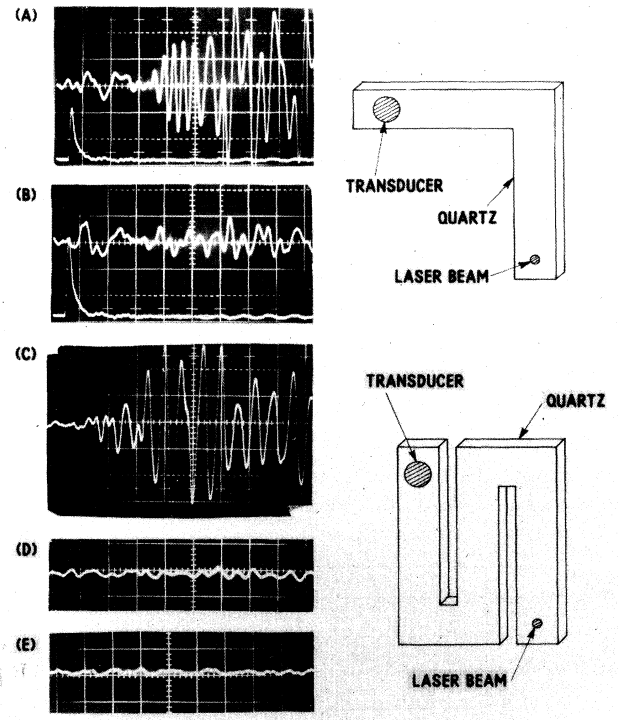

FIG. 11. Comparisons of two geometries for optoacoustic spectroscopy of powders. (A) and (C) show optoacoustic signals when the dye laser is tuned to the peak of an absorption line (no. 7) of Ho_2O_3 and (B) and (D) show corresponding signals when the dye laser is tuned away from the absorption peak. (E) shows the optoacoustic transducer output when the laser beam is blocked.

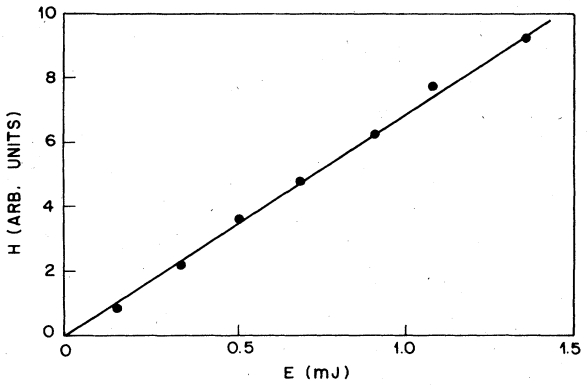

FIG. 12. Verification of the linearity of the OA signal amplitude H for various laser pulse energies (changed by the use of neutral density filters). This example is for benzene at a laser frequency of 18 810 cm^{-1} (peak of the seventh harmonic of the C–H stretch).

veniently done with liquid H_2O, which has a very rapidly changing β with temperature; indeed, β changes sign at 4 °C. Our observed OA signals at various temperatures are shown in Fig. 13. At 4 °C, a very weak OA signal is observed, as seen in Fig. 13(E), corresponding to weak absorptions at cell windows and noise due to electrical pickup. At lower or higher temperatures, OA signals due to water absorption are clearly seen, after a delay time due to acoustic propagation. We see from Fig. 13 that the OA signal changes sign at 4 °C; i.e., the signal (at early time) reverses phase as we follow it from above 4 °C to below 4 °C. (Later signals are contaminated by window absorptions and no clear phase reversal is seen). We have plotted the ratio of the OA signal to the known thermal expansion coefficient β of water in Fig. 14. We find that this ratio is a constant, independent of temperature, in agreement with Eq. (1), and implying that the other parameters such as the absorption coefficient α are, at most, very slowly changing with temperature.

V. EXPERIMENTAL RESULTS

In this section we review the results in linear and nonlinear spectroscopy that we have obtained so far with the pulsed OA detection technique described above. The purpose of this section is to exemplify how quantitative linear or nonlinear spectroscopy can be performed in cases where new physical information has been obtained. We note that small linear absorptions in liquids have been studied by other methods, e.g., by conventional long-path-length absorption spectroscopy (Stone, 1978), by wavelength modulation spectroscopy (Moses and Tang, 1977), by laser calorimetry (Callis, 1976), by Michelson-type double-arm absorption spectroscopy (Querry *et al.*, 1978), by

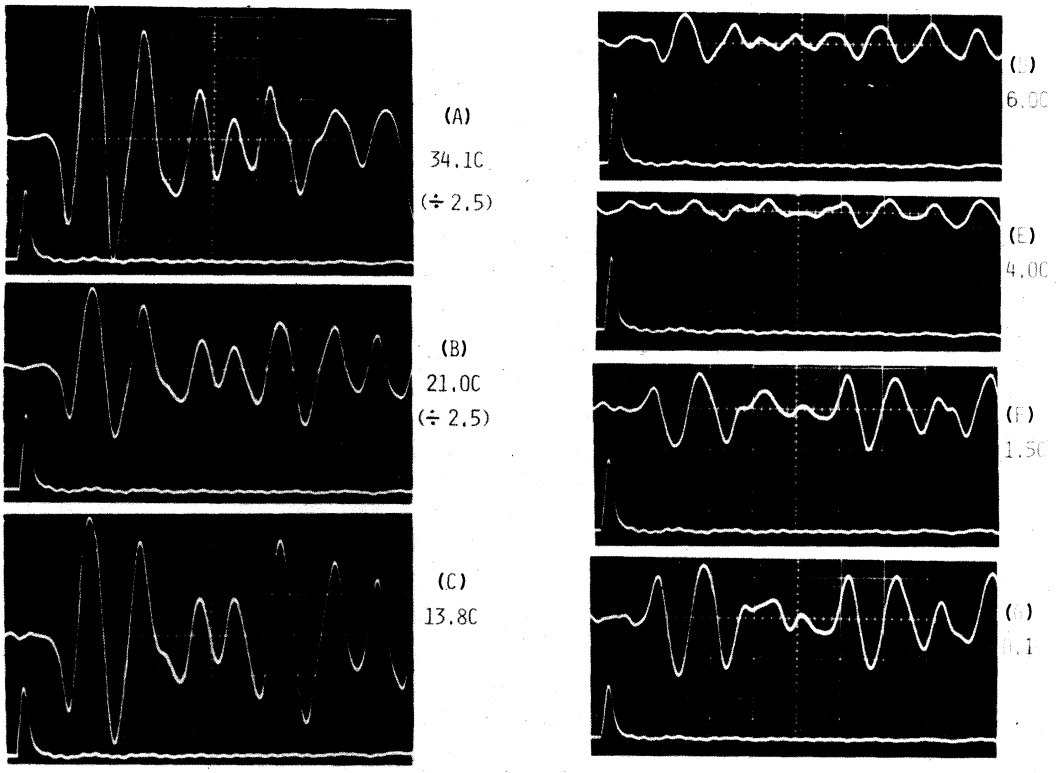

FIG. 13. Transducer output signal for water at various temperatures. In each of the scope pictures, the upper trace is the transducer output signal for liquid H_2O at the indicated temperature (in °C); the lower trace is the laser pulse detected by the pyroelectric detector. The laser frequency is fixed at 16 400 cm^{-1}. Horizontal scale is 5 μsec cm^{-1}. Vertical sensitivities are the same for all the pictures except (A) and (B), where the normal sensitivity is decreased by a factor of 2.5, as indicated. Note the phase reversal of the early part of the transducer output at 4 °C.

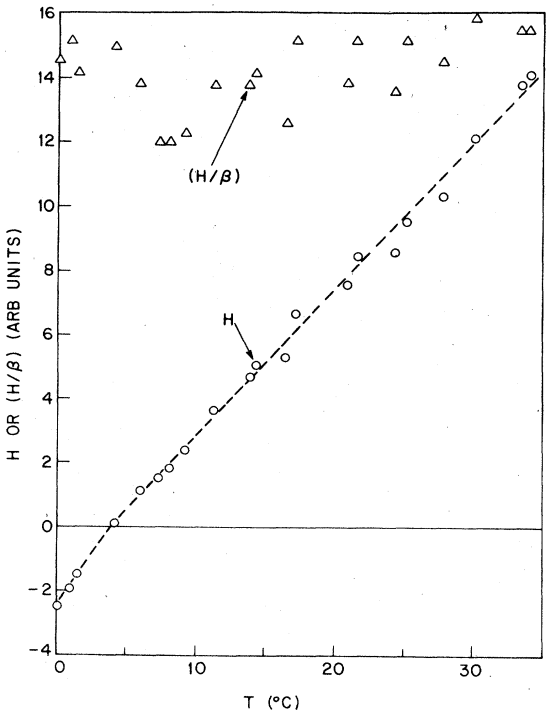

FIG. 14. Measured optoacoustic signal and the ratio of measured OA signal to known thermal expansion coefficient for water as a function of temperature.

thermal-lensing spectroscopy (Long *et al.*, 1976), and so on. References to these other methods of investigation have been made in our recent publication (Patel and Tam, 1979a) and these other methods will not be discussed here. In any case, we believe that the pulsed OA technique, in general, produces more accurate and/or reliable results compared to the other methods of investigation. For example, in the case of the optical absorption spectrum of liquid H_2O, other methods have yielded absorption coefficients (in the green spectral region) with mutual disagreements by as much as a factor of 10. Our OA results in water seem to be the most accurate up to date.

A. Linear spectroscopy

1. Water

Liquid water is a very transparent material in the visible region. Because of the fundamental and practical importance of water, many researchers have attempted to measure its optical absorption over the past century. However, this has remained a very challenging task, and results from different measurements typically disagree by factors of ~2 or more. Thus we see that all the conventional ways of measuring weak absorption, such as the optical absorption of water in the visible region, suffer from several difficulties: (a) If the extinction coefficient is being measured instead of absorption (as is done in most investigations), then the amount of scattering loss must be known. This is quite difficult in general, because liquid samples frequently contain microscopic particles that cause strong light scattering. (b) Absorption and reflection losses at windows are frequently hard to account for accurately. (c) Insufficient collimation, lateral displacements, reflections at cell walls, etc., of the light beam are frequent sources of errors. These problems are especially severe when long-path-length absorption cells are used.

Our pulsed OA technique specifically eliminates the above problems. Also, our choice of highly corrosion-resistant material for construction of our OA cell results in no contamination problems. This is verified from the fact that the same OA spectrum is obtained for a freshly distilled water sample as for a sample stored in the OA cell for several weeks. Furthermore, the high sensitivity obtainable with the pulsed OA technique enables us to obtain the first unambiguously accurate optical spectra of liquid H_2O and D_2O.

Figures 15 and 16 show our observed OA absorption spectra of light and heavy water, respectively, in the visible region. Detailed tabulation of the absorption coefficients is given in Table I (Tam and Patel, 1979b).

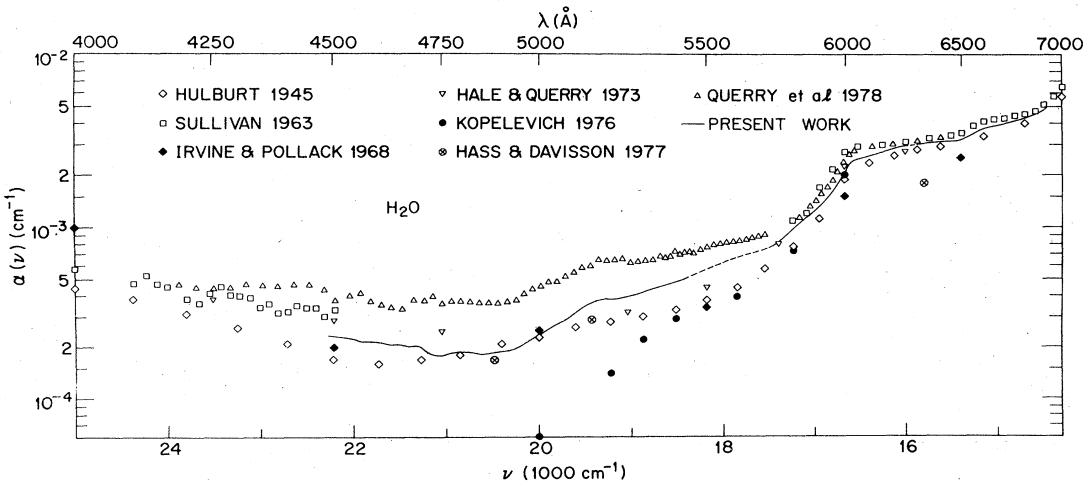

FIG. 15. Absorption spectra of distilled light water by optoacoustic determinations (shown by full line). The dashed parts are interpolations not covered by the tuning range of the laser dyes used. Also shown are some experimental data from other authors for comparisons. (See Hulburt, 1945; Sullivan, 1963; Irvine and Pollack, 1968; Hale and Querry, 1973; Kopelevich, 1976; Hass and Davisson, 1977; Querry *et al.*, 1978, for descriptions of their work.)

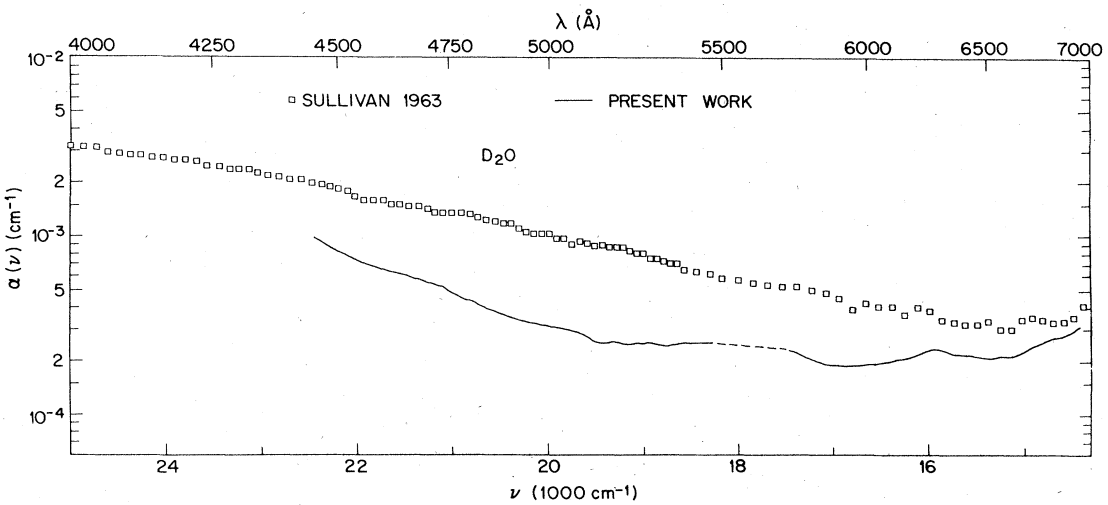

FIG. 16. Absorption spectra of distilled heavy water by optoacoustic determinations. Notations same as in Fig. 12.

TABLE I. Absorption coefficients of liquid water at 21.5 °C by laser optoacoustic spectroscopy.

ν (cm^{-1})	λ (nm)	α (H_2O) (10^{-4} cm^{-1})	α (D_2O) (10^{-4} cm^{-1})	ν (cm^{-1})	λ (nm)	α (H_2O) (10^{-4} cm^{-1})	α (D_2O) (10^{-4} cm^{-1})
22 400	446.3	2.38	9.50	18 700	534.7	4.39	2.40
22 300	448.3	2.33	8.68	18 600	537.5	4.53	2.48
22 200	450.4	2.30	8.11	18 500	540.4	4.80	2.49
22 100	452.4	2.27	7.69	18 400	543.5	5.00	2.50
22 000	454.4	2.21	7.27	18 300	546.3	5.28	2.50
21 900	456.5	2.14	6.96	17 400	574.5	8.05	2.22
21 800	458.6	2.13	6.68	17 300	577.8	8.99	2.10
21 700	460.7	2.11	6.46	17 200	581.2	10.07	2.01
21 600	462.9	2.06	6.17	17 100	584.6	11.07	1.91
21 500	465.0	2.06	6.03	17 000	588.0	12.32	1.89
21 400	467.2	2.00	5.77	16 900	591.5	13.77	1.86
21 300	469.4	2.05	5.60	16 800	595.0	15.89	1.86
21 200	471.6	1.84	5.41	16 700	598.6	19.25	1.88
21 100	473.8	1.77	5.20	16 600	602.2	23.2	1.92
21 000	473.1	1.79	4.74	16 500	605.9	24.8	1.97
20 900	478.4	1.86	4.51	16 400	609.6	25.7	2.00
20 800	480.7	1.86	4.39	16 300	613.3	26.7	2.03
20 700	483.0	1.84	4.09	16 200	617.1	27.7	2.09
20 600	485.3	1.81	3.83	16 100	620.9	28.8	2.22
20 500	487.7	1.86	3.70	16 000	624.8	29.6	2.28
20 400	490.1	1.89	3.51	15 900	628.7	30.0	2.28
20 300	492.5	1.93	3.39	15 800	632.7	30.4	2.20
20 200	494.9	2.00	3.22	15 700	636.7	31.0	2.15
20 100	497.4	2.16	3.19	15 600	640.8	31.0	2.15
20 000	499.9	2.33	3.10	15 500	645.0	31.4	2.14
19 900	502.4	2.50	3.05	15 400	649.2	32.3	2.06
19 800	505.0	2.70	2.98	15 300	653.4	33.1	2.12
19 700	507.5	2.88	2.89	15 200	657.7	36.1	2.12
19 600	510.1	3.13	2.72	15 100	662.1	37.9	2.15
19 500	512.7	3.48	2.54	15 000	666.5	38.7	2.26
19 400	515.4	3.65	2.50	14 900	670.9	39.5	2.40
19 300	518.0	3.75	2.55	14 800	675.5	40.8	2.54
19 200	520.7	3.80	2.46	14 700	680.1	42.6	2.69
19 100	523.5	3.87	2.48	14 600	684.1	45.1	2.74
19 000	526.2	3.97	2.48	14 500	689.2	47.6	2.90
18 900	529.0	4.09	2.48	14 400	694.2	52.6	3.20
18 800	531.8	4.27	2.41				

Several other measurements of the absorption coefficient of water obtained by methods other than OA are also indicated in Figs. 15 and 16. They represent better known results obtained in relatively recent years, and we see that some of these data disagree by factors as large as 10. The accuracy of our OA data is estimated as ±10%.

Figures 15 and 16 also clearly show the large differences in the absorption spectra of liquid H_2O and D_2O. The absorption in the red (say, at a frequency of ~15 380 cm^{-1} corresponding to a wavelength of ~6500 Å) is an order of magnitude larger than that by D_2O, and the absorption "knees" at 16 550 and 19 460 cm^{-1} in H_2O are absent in D_2O. This is because the major contribution to the optical absorption of H_2O in the red and *longer* wavelengths is due to overtones and combinations of the O–H vibrational modes. For example, the knees at 16 550 and 19 460 cm^{-1} are due to the fifth and sixth harmonics of the O–H stretch. The frequencies ν_n of the high nth harmonic are reasonably well fitted by the following simple anharmonic formula:

$$\nu_n(H_2O) = n(3620 - 63n)\ cm^{-1}. \tag{50}$$

In general the intensities of harmonic absorptions are smaller for higher harmonics. This is why the fifth harmonic of the O–H stretch is small in H_2O, and the sixth is even smaller. These high harmonics for D_2O lie in the near ir, since the O–D stretching frequency is smaller than the O–H stretching frequency by a factor of $\sqrt{2}$. Hence it is easy to understand why the red and near-ir absorption of D_2O should be much smaller than that for H_2O. Incidentally, this fact may be used to great advantage in dye laser technology, where water is very frequently used as a dye solvent because of its high specific heat and the small temperature dependence of the refractive index. In the red and near ir, the attractive properties of H_2O are offset by the not-insignificant absorption by H_2O itself. However, the use of D_2O should decrease the absorption by the solvent itself by more than an order of magnitude.

2. Transparent organic liquids

Almost all common pure organic liquids are "transparent" in the visible, and small absorption structures in this high-transparency region are frequently unsuspected or usually unmeasurable. As in the case of water, a major source of weak absorption structures is the high overtones of a fundamental or combination of vibrational modes. Higher overtones decrease rapidly in intensity, so that increasingly sensitive techniques are needed to examine the absorption profile of these overtones for increasingly high harmonics. Our pulsed OA technique is ideally suitable for the investigation of high-overtone profiles, and we have done this for benzene, methanol, acetone, and other common organic liquids.

Our observed OA spectra for benzene (Patel *et al.*, 1979) are shown in Fig. 17, which shows the profile of the sixth, seventh, and eighth harmonics of the C–H stretch. Only the sixth harmonic profile has previously been quantitatively studied by other means; these previous means include thermal-lensing spectroscopy (Long *et al.*, 1976), wavelength-modulation spectroscopy (Moses and Tang, 1977), and long-pathlength spectroscopy utilizing liquid-filled hollow optical fibers (Stone, 1978). A comparison of these other previous studies of the sixth harmonic in benzene is shown in Fig. 18, where all absorption profiles are normalized to the same height to facilitate comparison.

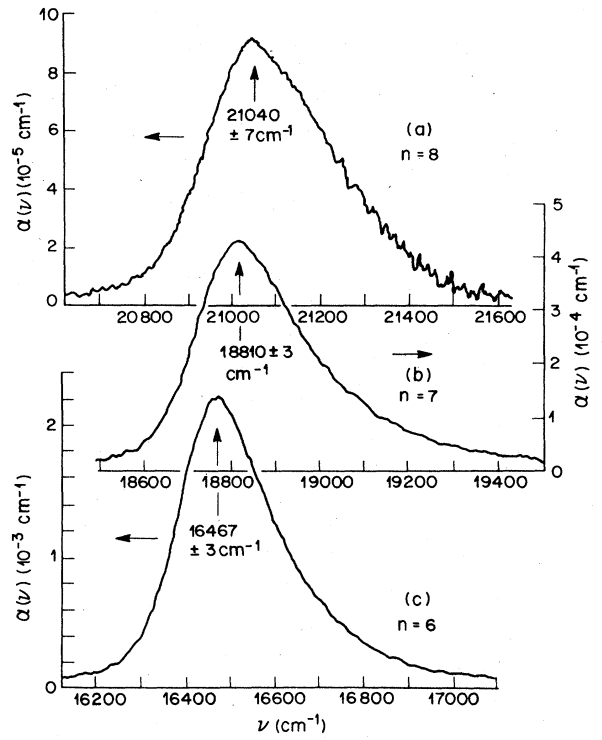

FIG. 17. Measured absorption profiles of the $n = 8$ to $n = 6$ harmonics of the C–H stretch in liquid benzene by laser OA spectroscopy.

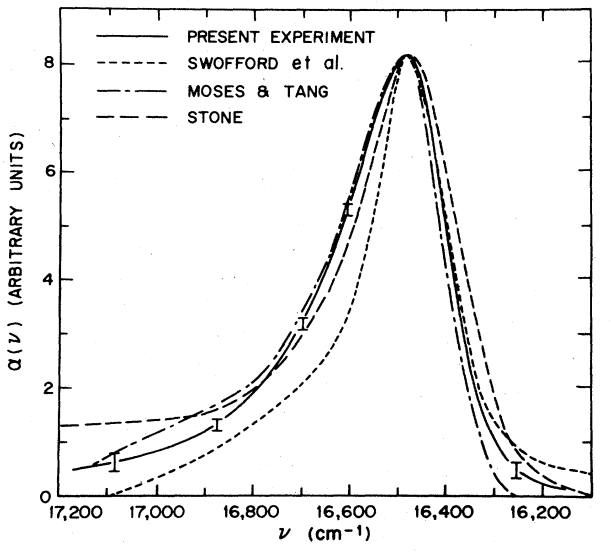

FIG. 18. Comparison of the absorption profile due to the sixth harmonic of the C–H stretch presently observed, with results obtained by other methods (see Long *et al.*, 1976; Moses and Tang, 1977; and Stone, 1978, for description of other methods used).

Significant disagreements exist (Patel *et al.*, 1979) between the optoacoustic absorption data and some of the previous data; however, we believe that our profile, with its absolute scale (see Fig. 17) is the most reliable so far.

The detection of the high overtones in benzene allows us to examine the systematic trend of the series of overtones. The frequency ν_n of the nth harmonic of the C–H stretch is found to be surprisingly well fitted by the following anharmonic formula:

$$\nu_n(C_6H_6) = n(3090.5 - 57.6n) \text{ cm}^{-1}. \quad (51)$$

It may seem curious that a high harmonic remains a well-defined absorption feature, since the large number of possible combinations of vibrational modes (of a wide range of energies because of anharmonicity) may lead one to think that a high harmonic absorption profile would be much more spread out than that actually observed. The reason is that a high overtone is best described by a local mode (where all the vibrational excitation is localized in one bond) rather than by normal modes (where linear combinations of vibrations in various bonds are used). The current research on local mode theory is given, e.g., by Henry (1968, 1977) and co-workers (Hayward and Henry, 1976; Hayward *et al.*, 1973).

As mentioned earlier, the absorption intensities of higher overtones rapidly drop at higher n. The magnitude of the peak absorption, and the absorption linewidth (full width at half maximum) as functions of n are plotted in Figs. 19 and 20, respectively. No satisfactory theoretical understanding of these functional dependences is available at present. Figure 20 shows that linewidths of the harmonic series broaden linearly with n. Further, Fig. 21 shows the assymmetry parameter, defined as the ratio of half-width at half maximum (HWHM) on the blue side to that on the red side, as a function of n where the harmonic absorptions appear as a single component. The liquid-phase linewidth data are in sharp contrast to the gas-phase linewidths, which are roughly a factor of 3 narrower than in the liquid case, and slowly diminish with increasing n for $n = 5$, 6, and 7 [see Patel and Tam (1979b) for a comparison with the work of Reddy, Bray, and Berry (1978)]. The large difference between the gas and liquid cases must be partially due to the proximity of benzene molecules in the liquid. This is seen when liquid benzene is diluted in CCl_4; the absorption profile (Fig. 22) of the sixth harmonic becomes narrower, more blue-shifted, and more symmetrical as dilution

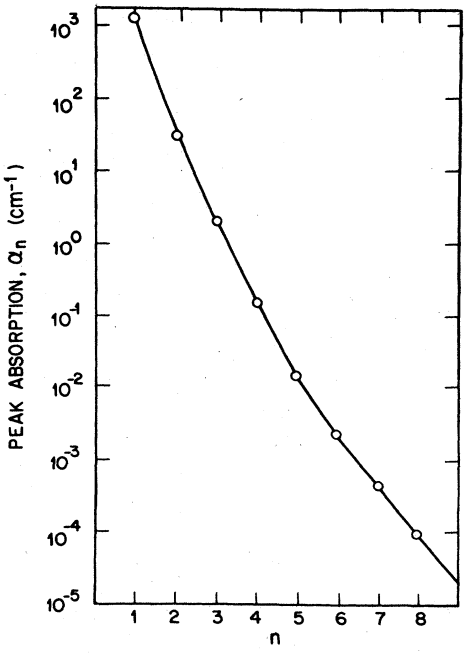

FIG. 19. Observed variations of peak absorption coefficient α_n with n.

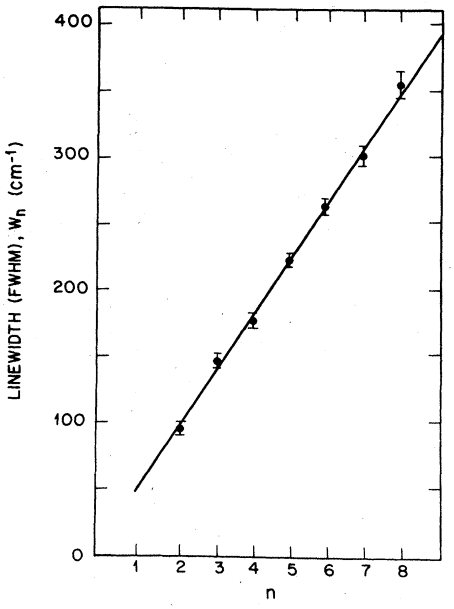

FIG. 20. Observed linewidth (full width at half maximum) W_n for the nth harmonic of the C–H stretch in liquid benzene as a function of n.

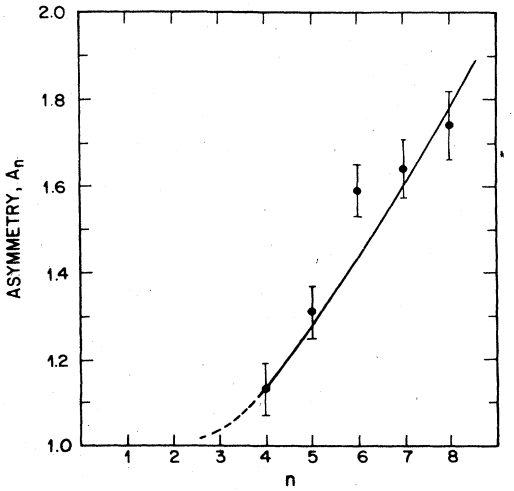

FIG. 21. Measured asymmetry parameter (ratio half-width at half-height on the high-frequency side of the peak to that on the low-frequency side of peak) for the overtone spectra of benzene as a function of n.

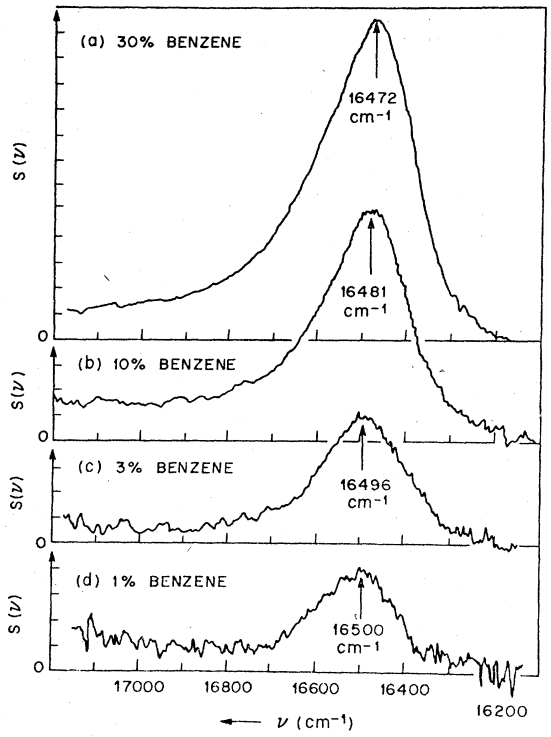

FIG. 22. Effect of dilution (of benzene in CCl_4) on the profile of the sixth harmonic in benzene. $S(\nu)$ is the absorption coefficient in arbitrary linear units. The concentrations of benzene by volume in the solution are indicated. Positions of the absorption peaks, obtained by averaging over several scans, are given.

increases, i.e., the profile tends toward the gas-phase case as dilution increases. Table II summarizes the measured line center, linewidth, and assymmetry parameter for the sixth harmonic of benzene as a function of dilution in CCl_4. Incidentally, we can estimate from the signal-to-noise ratio seen in Fig. 22(d) for the 1% dilution case that we can presently detect absorption coefficients *at least* as small as 10^{-6} cm^{-1}.

3. Thin liquid films

In the above discussions, we have demonstrated that the pulsed OA technique represents a powerful method for detecting weak absorptions. Since fractional absorption is equal to the product of the absorption coefficient α and the path length l, weak absorption can result either from small α (as in the above cases) or from small l. For the case of benzene, we have demonstrated that we can detect a fractional absorption of $\lesssim 10^{-6}$. If we extrapolate this result to the case of short path length, we may estimate that we can detect absorption features due to a thickness of $l \sim 10^{-8}$ cm if the absorption coefficient α is $\sim 10^{2}$ cm^{-1}, a moderately large value. This would clearly open up a lot of possibilities in thin-film spectroscopy and surface science.

The above estimates of our ability to measure thin-film absorption may be too optimistic, because (a) the effect of scattered laser light by the film may create serious problems, and (b) there may be no good way to directly couple the transducer to the film, as in the bulk liquid cases previously discussed. However, if the film is mounted firmly onto a transparent substrate (e.g., by sandwiching the film between the substrate and a cover plate), then the pulsed OA effect in the film can launch both bulk as well as surface acoustic waves into the substrate. As discussed in Sec. III.D, the acoustic waves can be efficiently detected by a piezoelectric transducer directly coupled to the substrate at a distance ~10 cm away from the laser-irradiated region, thus minimizing light scattering onto the transducer. Light scattering can further be reduced by a suitable shape of the substrate, i.e., a shape with bends. These considerations have led us to a new type of pulsed OA "cell," shown in Fig. 6. We found that this cell is useful both for liquid films and for powder films, clamped between the quartz plates.

To test the usefulness of this arrangement for liquid films, we have examined (Patel and Tam, 1980) the absorption spectra of film of rare-earth chloride aqueous solutions, of concentration about 1 gm cm^{-3}. Some results are shown in Fig. 23. From these studies, we estimate that we can presently detect films that cause a fractional absorption of 10^{-5}. This clearly shows that absorption features due to monolayers on a transparent substrate can be detected with the pulsed optoacoustic spectroscopy technique if the absorption coefficient of the molecules in the monolayer exceeds 10^{3} cm^{-1}, and if the substrate is of high enough transparency.

TABLE II. Line center position, linewidth (FWHM), and symmetry of the sixth overtone of the C–H stretch in benzene as a function of benzene dilution in carbon tetrachloride. Corresponding data for gas-phase results are also given.

Dilution (C_6H_6 in CCl_4)	Position (cm^{-1})	Linewidth (cm^{-1})	Asymmetry
1.0	16 467 ± 3	278 ± 9	1.55
0.3	16 472 ± 3	259 ± 9	1.49
0.3	16 481 ± 3	228 ± 9	1.41
0.03	16 496 ± 3	222 ± 9	1.13
0.01	16 500 ± 3	220 ± 20	1.09
Gas phase	16 550	94	1.0

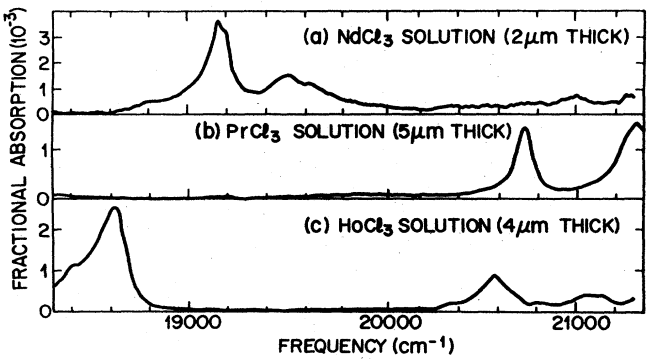

FIG. 23. OA absorption spectra of thin films of $NdCl_3$, $PrCl_3$, and $HoCl_3$ aqueous solutions.

The idea of external coupling of a transducer to a sample for optoacoustic detection (Fig. 6) has been extended by Tam and Patel (1980) to construct an extremely corrosion resistant optoacoustic cell for liquids. Such arrangements have been shown by Voigtman *et al.* (1981) to be well suited to detect trace amounts of dyes, drugs, and biochemicals.

4. Powders and solids

One attractive feature of OA spectroscopy is that absorption spectra of highly light-scattering materials (e.g., powders) can be examined. This advantage has been frequently emphasized in conventional OA techniques (Monohan and Nolle, 1977; Rosencwaig, 1977; Rosencwaig, 1978). However, the "immunity" of conventional OA techniques (utilizing an enclosed gas cell containing the powder, a gas-phase microphone, chopped cw light beam, and phase-sensitive detection) to light scattering is often exaggerated. In fact, strong light scattering can cause optical absorption at cell walls and at the microphone, producing spurious signals (McClelland and Kniseley, 1976). Furthermore, most of the conventional OA powder measurements have been done with samples thick enough so that all the incident light is absorbed. This poses the problem of uncertain optical intensity dependence on the penetrating depth, since strong light scattering causes enhanced light intensity nearer the top layer of the powder sample. There are also subtle problems with chopping frequency dependence and signal saturation in optically thick samples. Thus, although numerous authors have used the conventional OA technique to examine powder spectra, few quantitative data producing new information have been reported. For example, reported OA data on Ho_2O_3 powders have been numerous (Blank and Wakefield, 1979; Eaton and Stuart, 1978; Rosencwaig, 1977), but only the recent data of Shaw (1979) are of respectable quality.

During our efforts to overcome the above problems we discovered (Tam and Patel, 1979c) that the thin-film apparatus shown in Fig. 6 is ideally suited for OA spectroscopy of thin layers of powders. The fine powder suspension in a clear viscous liquid is clamped between the quartz plates, and the OA signal generated in the powder couples very efficiently into the liquid and then into the substrate. The powder film is optically thin, so that we do not encounter complications due to total light absorption (like the signal saturation problems mentioned above).

Examples of OA spectra of rare-earth oxide powders, Ho_2O_3, Dy_2O_3, and Er_2O_3, are shown in Figs. 24–26, respectively. The laser bandwidth (2 cm^{-1}) at present is sufficiently small to resolve all the spectral lines (of width ~10 cm^{-1}) of the room-temperature powdered crystals in the spectral range investigated. More detailed investigations can be made possible by cooling the powder to cryogenic temperatures (when linewidth can be $\lesssim$0.1 cm^{-1}), and performing OA spectroscopy using a dye laser with suitable intracavity etalon to narrow the laser linewidth.

We have identified (Tam and Patel, 1979c) the lines for Dy_2O_3 (Table III) and Er_2O_3 (Table IV) oxide powders shown in Figs. 25 and 26. The lines are due to transitions between Stark components of the ground state and Stark components of an excited state. We have derived the ground-state Stark splittings and the excited-state Stark splittings in the powdered crystals at room temperature. These data are shown in Table V and Table VI for Dy_2O_3 and Er_2O_3, respectively. More accurate splittings can be derived by cooling the powders. Our work seems to provide the first example that quantitative spectroscopy of ions in finely powdered crystals can be performed by the OA technique. We would like to mention, however, that while we have so far established a capability for obtaining high-resolution absorption spectra of powders, we have left the questions of linearity range unanswered. Unlike the case of liquids where we have rigorously checked to assure linearity of the optoacoustic signal as a function of the absorption coefficient α (to make sure that αl is small), no OA signal generation theory for powder samples has yet been put forward. This area is likely to become very important, and additional work, both theoretical and experimental, is needed.

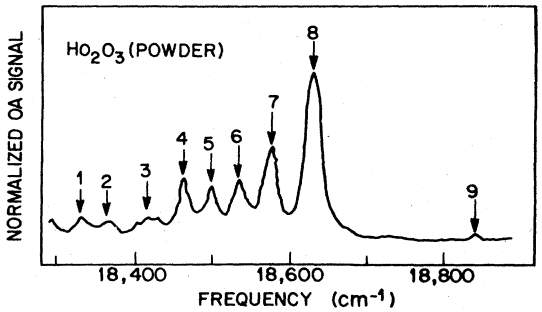

FIG. 24. OA absorption spectrum in the green-blue region for Ho_2O_3 powder at 25 °C. Prominent spectral lines are marked.

Sam and Shand (1979) have used a slightly different technique for carrying out pulsed optoacoustic spectroscopy of weakly absorbing solids. Instead of using a piezoelectric transducer that is directly attached to the solid, they immerse the solid sample in a transparent liquid and detect the optoacoustically generated pressure pulse using a submerged piezoelectric transducer, as done by Patel and Tam (1979a) for the measurements of weak optical spectra of liquids. This extension of the Patel and Tam (1979a) technique, which they call the SLT (solid-liquid-transducer) technique, is reminiscent of the photoacoustic spectroscopy technique described by Harschbarger and Robin (1973) and

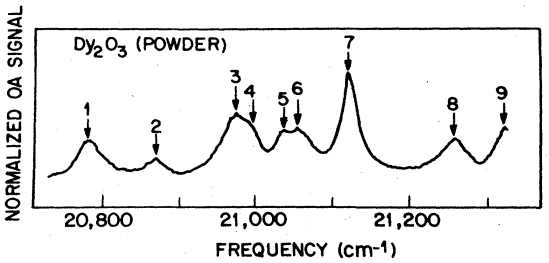

FIG. 25. Optoacoustic spectrum in the blue-green region for Dy_2O_3 powder at 25 °C. Identifiable peaks are indicated.

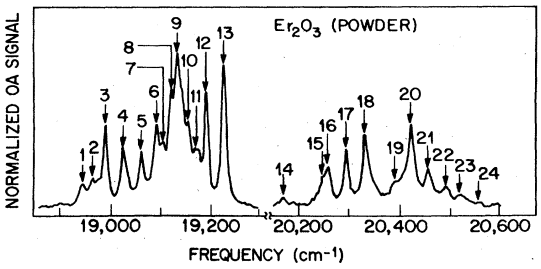

FIG. 26. Optoacoustic spectrum in the blue-green region for Er_2O_3 powder at 25 °C. Prominent peaks are indicated.

Rosencwaig (1973), which was an extension of the highly successful gas-phase optoacoustic spectroscopy technique that utilized microphones as transducers (Kreuzer, 1971; Kreuzer and Patel, 1971) to condensed matter. In the photoacoustic spectroscopy scheme (as it has come to be known) of Harshbarger and Robin (1973) and Rosencwaig (1975), the photo-thermal signal generated in a solid (for example) is coupled to a gas and detected with a sensitive microphone, and is dubbed the SGM (solid-gas-microphone) technique. In the SGM case, there are two origins of sound generation: (a) primary OA signal generation in the solid, with the signal only very weakly transmitted across the gas-solid interface, and (b) secondary photoacoustic signal generation in the gas due to thermal coupling with the illuminated solid surface. In SGM detection, the detected signal is mainly due to source (b) (see, for example, Rosencwaig and Gersho, 1976; McDonald and Wetsel, 1978), and the poor acoustic coupling between solid and gas is not an issue. However, in other schemes where primary acoustic signals are monitored, acoustic impedances of the solids or liquids involved and the coupling schemes used are important factors to consider. For example,

$$Z_{ac}=\rho v_a \tag{52}$$

gives

$$Z_{ac}(\text{helium gas})=5\ \text{gm cm}^{-2},$$
$$Z_{ac}(\text{solid})\approx 8\times 10^5\ \text{gm cm}^{-2},$$
$$Z_{ac}(\text{liquid})\approx 2\times 10^5\ \text{gm cm}^{-2}.$$

TABLE III. Lines of the $^4F_{9/2}\leftarrow{}^6H_{15/2}$ absorption multiplet presently observed in Dy_2O_3 powder at 25 °C. ν_{exp} is the observed peak position (cm^{-1}), I is the intensity (arb. unit), W is full width at half maximum (cm^{-1}), T is the transition identified, and ν_{calc} is the calculated peak position (cm^{-1}) according to the energy levels presently fitted, as given in Table V.

No.	ν_{exp}	I	W	T	ν_{calc}
1	10 780	13	40	$F_1\leftarrow H_3$	20 780
2	20 868	6	31	$F_3\leftarrow H_3$	20 866
3	20 971	20	40	$F_1\leftarrow H_2$	20 971
4	20 994	10	22	$F_2\leftarrow H_2$	20 994
5	21 038	10	25	$F_1\leftarrow H_1$	21 038
6	21 056	10	36	$F_3\leftarrow H_2$	21 057
7	21 121	35	27	$F_3\leftarrow H_1$	21 124
8	21 260	13	43	$F_4\leftarrow H_2$	21 259
9	21 325	16	34	$F_4\leftarrow H_1$	21 326

TABLE IV. Lines of the $^2H_{11/2}\leftarrow{}^4I_{15/2}$ and $^4F_{7/2}\leftarrow{}^4I_{15/2}$ absorption multiplets presently observed in Er_2O_3 powder at 25 °C. Notations are same as in Table III, except that I_n, H_n, and F_n denote sublevels of $^4I_{15/2}$, $^2H_{11/2}$, and $^4F_{7/2}$, respectively, with energy increasing for larger n. These energy sublevels are tabulated in Table VI.

No.	ν_{exp}	I	W	T	ν_{calc}
1	18 943	12	10	$H_1\leftarrow I_4$	18 944
2	18 963	10	8	$H_2\leftarrow I_3$	18 963
3	18 990	60	9	$H_3\leftarrow I_3$	18 988
4	19 025	40	10	$H_3\leftarrow I_2$	19 025
5	19 062	34	8	$H_3\leftarrow I_1$	19 063
6	19 093	28	10	$H_4\leftarrow I_4$	19 094
7	19 107	5		$H_4\leftarrow I_3$	19 107
8	18 122	25	6	$H_5\leftarrow I_4$	19 124
9	19 135	100	10	$H_5\leftarrow I_3$	19 137
10	19 157	8		$H_6\leftarrow I_3$	19 157
11	19 174	8		$H_5\leftarrow I_2$	19 174
12	19 195	90	10	$H_6\leftarrow I_2$	19 194
13	19 232	140	10	$H_6\leftarrow I_1$	19 232
14	20 168	9	20		
15	20 247	7	10	$F_1\leftarrow I_4$	20 246
16	20 259	30	12	$F_1\leftarrow I_3$	20 259
17	20 295	48	10	$F_1\leftarrow I_2$	20 296
18	20 334	60	14	$F_1\leftarrow I_1$	20 334
19	20 395	5		$F_2\leftarrow I_2$	20 396
20	20 426	70	14	$F_3\leftarrow I_3$	20 425
21	20 462	22	12	$F_3\leftarrow I_2$	20 462
22	20 496	10	20		
23	20 522	6		$F_4\leftarrow I_2$	20 522
24	20 560	3		$F_4\leftarrow I_1$	20 560

The reflection of a sound wave at an interface between two materials having dissimilar acoustic impedances is given by

$$R=\left(\frac{Z_{ac}(1)-Z_{ac}(2)}{Z_{ac}(1)+Z_{ac}(2)}\right)^2. \tag{53}$$

Thus we see that the acoustic reflections $R_{g\text{-}s}$ and $R_{s\text{-}l}$ gas-solid and liquid-solid interfaces, respectively, are (typically)

$$R_{g\text{-}s}\approx 0.999\,91 \tag{54}$$

and

$$R_{s\text{-}l}\approx 0.56. \tag{55}$$

TABLE V. Energy levels of the lower Stark sublevels in the ground state $^6H_{15/2}$ and in an excited state $^4F_{9/2}$ of Dy^{3+} in Dy_2O_3.

State	Sublevel	Energy (cm^{-1}) This work	Energy (cm^{-1}) Henderson *et al.* (1967)
$^6H_{15/2}$	H_2	67	74
	H_2	67	74
	H_3	258	261
$^4F_{9/2}$	F_1	21 038	21 040
	F_2	21 061	21 064
	F_3	21 124	21 131
	F_4	21 326	21 339

TABLE VI. Energy levels of the lower Stark sublevels in the ground state $^4I_{15/2}$, and of the Stark sublevels in the excited states $^2H_{11/2}$ and $^4F_{7/2}$ of Er^{3+} in Er_2O_3.

State	Sublevel	Energy (cm^{-1}) This work	Energy (cm^{-1}) Gruber *et al.* (1966)
$^4I_{15/2}$	I_1	0	0
	I_2	38	38
	I_3	75	75
	I_4	88	88
$^2H_{11/2}$	H_1	19 032	19 033
	H_2	19 038	19 040
	H_3	19 063	19 067
	H_4	19 182	19 182
	H_5	19 212	19 213
	H_6	19 232	19 235
$^4F_{7/2}$	F_1	20 334	20 336
	F_2	20 434	20 435
	F_3	20 500	20 500
	F_4	20 560	20 561

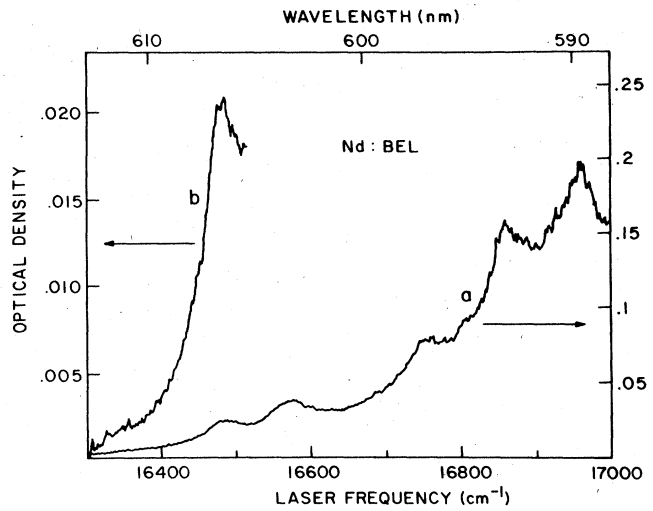

FIG. 27. Optoacoustic absorption spectrum of Nd : BEL measured using the solid-liquid-transducer technique. The sample was immersed in CCl_4 (after Sam and Shand, 1979).

Thus we can see that a sound wave has a transmission factor of $\sim 10^{-5}$ across a solid-gas interface, and thermal coupling between the solid and gas generally dominates in the SGM scheme. On the other hand, in OA experiments where the primary acoustic signal is measured, sound coupling must be optimized. In this consideration, the SLT scheme is not as efficient as the attached-transducer scheme since the acoustic signal generated in the solid has to be transmitted to the liquid in which it is immersed, and further the sound wave in the liquid has to be launched into the piezoelectric transducer for detection. Thus we have to contend with two solid-liquid interfaces giving a total transmission coefficient of $(1-R_{s-l})^2 \approx 0.19$ for transferring an acoustic signal from the solid sample to the piezoelectric transducer. The attached-transducer scheme, on the other hand, will have an acoustic signal transmission factor of $\gtrsim 0.9$. Hence the SLT scheme is much better than the SGM scheme as far as acoustic coupling is concerned, but still falls short of the attached-transducer technique. Sam and Shand (1979), however, suggest that the SLT scheme may be simpler to use for relative and rapid characterization of many different materials.

An example of pulsed optoacoustic spectroscopy based on the SLT scheme is the measurement of the absorption spectra of $Nd:La_2Be_2O_5$ (Nd:BEL) crystal with one atomic percent doping. The solid sample is suspended in a liquid optoacoustic cell directly above the piezoelectric transducer. The liquid, of course, has to be sufficiently transparent in the spectral region of interest. Sam and Shand used CCl_4, which has a very low absorption coefficient $\lesssim 10^{-6}$ cm^{-1} in the visible region. Figure 27 shows one of the spectra reported by Sam and Shand for Nd:BEL in the 16 300 to 17 000 cm^{-1} region. From the signal-to-noise ratio, they estimate a capability of measuring down to an absorption coefficient of $\sim 10^{-5}$ cm^{-1}; however, Fig. 27 indicates that in a Nd:BEL/CCl_4 system it would be difficult to measure an absorption coefficient smaller than $\sim 10^{-4}$ cm^{-1}.

One advantage of the SLT scheme is the lack of scattered light at the liquid-solid interfaces due to a good (but not perfect) refractive index match. Hence surface preparation may not be very crucial. However, the time gating scheme using a zig-zag substrate and direct attached-transducer scheme described for the study of powders (above) eliminates the scattering problem anyway. Thus the refractive index matching capability may be outweighed by a more serious problem of finding sufficiently transparent liquids that do not attack and dissolve the solid samples.

B. Nonlinear spectroscopy

As mentioned in Sec. IV, the use of a pulsed laser source, with its high peak power and low duty cycle (thus preventing significant heating of the sample), permits OA nonlinear spectroscopy to be readily performed. By nonlinear spectroscopy we mean spectroscopic studies of processes involving interaction of more than one photon. In these studies it is usually necessary to have high optical intensities. However, the intensities must be kept sufficiently low so that runaway self-action effects are not generated. For example, effects like self-focusing or stimulated Raman scattering originating from amplification of spontaneous emissions need to be prevented in a study of two-photon absorption or of Raman-gain spectroscopy. Hence the choice of a flash-lamp-pumped dye laser as the light source for nonlinear OA spectroscopy is quite appropriate in many cases. The laser pulse energy of ~1 mJ and duration ~1 μsec is usually focused to a spot size $\sim 10^{-4}$ to 10^{-5} cm^2 in our nonlinear spectroscopy studies. Thus the laser intensity is $\sim 10^7$ to 10^8 W cm^{-2}, and is well below the onset of self-action effects that may interfere with the studies. Another effect that one needs to be cautious about when dealing with a high-intensity laser beam is electrostriction (Bebchuk *et al.*, 1978, Brueck *et al.*, 1980). This effect is due to a positive or negative polarizability

of the molecules in the sample, causing the molecules to move towards or away from regions of higher optical intensities. The electrostriction effect is proportional to the laser intensity, and may interfere with the nonlinear optical studies if we use laser pulses of shorter duration but keep the pulsed energy constant. (See discussion of the electrostriction effect in Sec. II.D.)

Few nonlinear OA spectroscopy studies of condensed matter have been reported in the literature. This may be due to a lack of sensitivity (nonlinear absorption effects are usually very weak) without the use of a pulsed laser in the OA studies performed so far. We show here that weak nonlinear absorptions can be readily detected with the pulsed OA technique, as shown by our examples on two-photon absorption and Raman-gain spectroscopy. Such OA investigations have not been reported previously. It is clear that many more new nonlinear spectroscopy investigations of condensed matter are now possible, because of the high sensitivity of the pulsed OA technique. Furthermore, OA detection is frequently the preferred detection method for absorption in condensed matter, rather than fluorescence detection; this is because fluorescence is often quenched in condensed matter (but not in dilute gases).

1. Two-photon absorption

We have performed (Tam and Patel, 1979b) the first quantitative OA two-photon absorption spectroscopy of liquids. We have studied the two-photon electronic absorption arising from the $^1B_{2u} \leftarrow {}^1A_{1g}$ transition in benzene, which is symmetry forbidden, but becomes allowed in two-photon absorption by vibronic mixing. The forbidden nature of this transition results in a small two-photon absorption cross section σ throughout this band, and σ is always smaller than 10^{-51} cm^4 sec molecule^{-1} photon^{-1}. Fully allowed two-photon transitions usually have cross sections that are 2–3 orders of magnitude larger. However, the optoacoustic technique is adequate even for weak two-photon transitions.

Experimentally observed two-photon OA spectra are shown in Fig. 28, for linear and circular laser polarizations. To obtain these data, the OA cell (Fig. 4) is filled with distilled spectro-grade benzene, and a lens with a focal length of 5 cm is used to focus the dye laser beam at the center of the cell, as shown in Fig. 29. Multiple distillation of the commercially available benzene was seen to be necessary to eliminate suspended particles which were seen to give rise to large extraneous noise output, if the particles are irradiated by a focused light beam. The laser focus should be vertically in front of the center of the transducer diaphragm for optimum detection efficiency. This is because the source of acoustic energy is now nearly a point source near the focus, rather than a line source as in the linear absorption cases. Experimentally, this fine adjustment is performed by moving the lens towards or away from the cell, so as to optimize the transducer signal observed on an oscilloscope.

The two-photon OA signal intensity is found to be nearly independent of the focal length of the lens used, if the laser focus is adjusted to be directly in front of the transducer. This is verified for focal lengths in the range of 8 to 2 cm. The reason is that a shorter focal length results in a higher laser intensity but a correspondingly shorter confocal distance, and these two effects nearly counterbalance each other. We have also verified that the two-photon absorption peaks (all except X) in Fig. 28 have intensities proportional to the square of the laser pulse energy. Hence the data of Fig. 28 have been normalized to the square of the pulse energy. (Use of the minicomputer for digitizing signals A and B, in Fig. 28, facilitates the normalizing of the OA signal by the square of the laser pulse energy.) The peak X varies linearly with the laser intensity and arises from the seventh harmonic absorption in benzene as discussed in Sec. V.A.2.

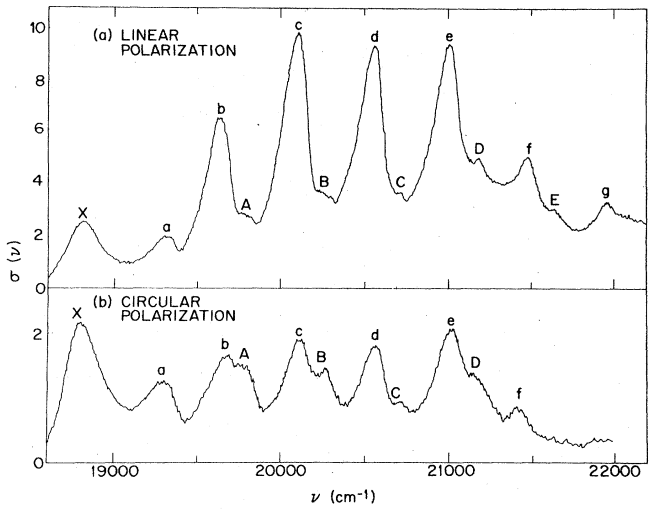

FIG. 28. Spectra of the two-photon $^1B_{2u} \leftarrow {}^1A_{1g}$ band in liquid benzene. $\sigma(\nu)$ is the two-photon absorption cross section in 10^{-52} cm^4 sec molecules^{-1} photon^{-1}, and ν is the single-photon frequency in cm^{-1}. Note that the absorption peak at 18 810 cm^{-1} is not a member of this band, but is the peak of the seventh harmonic of the C–H stretch. The relative heights of the different vibrational transitions are quite different for (a) linear laser polarization and (b) circular laser polarization.

Vibrational intervals and electronic origin can be derived (Tam and Patel, 1979b) from the data of Fig. 28. These are summarized in Table VII, which identifies

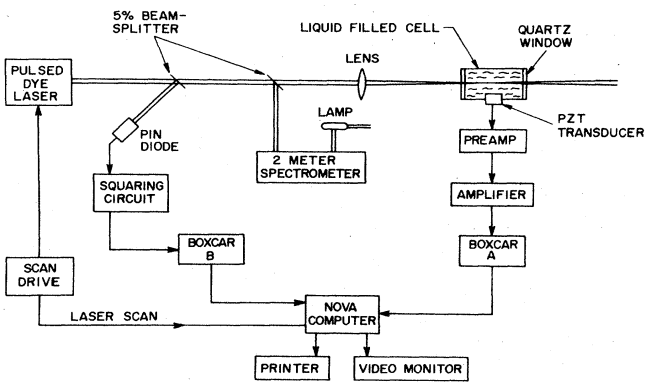

FIG. 29. Schematic of experimental arrangement for measuring two-photon optoacoustic spectra of liquids. The lens focal length is typically 5 cm.

TABLE VII. Observed peaks by Two-Photon Optoacoustic Spectroscopy, TPOAS, of the $^1B_{2u} \leftarrow {}^1A_{1g}$ band in liquid benzene. All values given are for linearly polarized laser light. Listed columns show laser frequency and notation of an absorption peak, the exponent of its laser energy dependence (±0.1), two-photon absorption cross section, vibrational energy in the B_{2u} state (we set the electronic origin at 37 724 cm^{-1} in the liquid phase), identification of the transition, and calculated position (above the electronic origin) of the absorption peak assuming gas-phase vibrational constants.

Observed peaks Frequency ν (cm^{-1})	Legend	Power dependence	Cross section [a]	$2\nu - 37\,724$ (cm^{-1})	Identification [b]	Calculated [c] position (cm^{-1})
18 810	X	1			1-*ph* 7th harm of C–H [d]	
19 323	a	2	2.1	922	18_0^1	923
19 644	b	2	6.6	1564	14_0^1	1564
19 792	A	2	1.5	1860	$18_0^1 1_0^1$	1843
20 106	c	2	10	2488	$14_0^1 1_0^1$	2488
20 241	B	2	1.8	2758	$14_0^1 10_0^2$	2731
					$18_0^1 1_0^2$	2770
20 569	d	2	9.2	3414	$14_0^1 1_0^2$	3414
20 690	C	2	2.1	3656	$14_0^1 10_0^2 1_0^1$	3656
21 031	e	2	9.0	4338	$14_0^1 1_0^3$	4333
21 047	Y	1			1-*ph* 8th harm of C–H [e]	
21 139	D	2	3.4	4554	$14_0^1 10_0^2 1_0^2$	4562
21 487	f	2	4.8	5250	$14_0^1 1_0^4$	5256
21 627	E	2	1.7	5530	$14_0^1 10_0^2 1_0^3$	5485
21 957	g	2	3.1	6190	$14_0^1 1_0^5$	6179

[a] 10^{-52} cm^4 $molecule^{-1}$ $photon^{-1}$ sec. The relative values of these cross sections are accurate to ±10% for the bigger peaks. The uncertainty in the absolute scale is a factor of 3 (see Tam and Patel, 1979a).
[b] Using Wilson's notation (Wilson, 1934).
[c] Using Wunsch *et al.*'s constants (Wunsch, Neusser, and Schlag, 1975a, 1975b).
[d] Patel and Tam, 1979b.
[e] Patel, Tam, and Kerl, 1979.

the vibronic origin of each of the peaks and gives accurate cross-section values for them. While the vibrational intervals are nearly identical to those known for benzene in the gas phase, the electronic origin for the band $^1B_{2u} \leftarrow {}^1A_{1g}$ is quite different. The electronic origin in the gas phase is known to be 38 086 cm^{-1}, in contrast to our value of 37 724 cm^{-1} for the liquid benzene case (see Tam and Patel, 1979b, for details). No quantitative explanation for this large red shift in the electronic origin is available at present.

We can also derive quantitative values for the two-photon cross sections σ for the present case by comparing (Tam and Patel, 1979b) the intensity of the two-photon transition with that of the one-photon transition (seventh harmonic of the C–H stretch) at 18 810 cm^{-1}, shown in Fig. 28. The absorption coefficient at 18 810 cm^{-1} is already measured by us to be 4.3×10^{-4} cm^{-1}, as seen from Fig. 17. We thus obtain an absolute scale for the two-photon spectra shown in Fig. 28. We may estimate from the signal-to-noise ratio in Fig. 28 that two-photon cross sections as small as 10^{-53} cm^4 sec $molecule^{-1}$ $photon^{-1}$ can be detected at present.

We also note from Fig. 28 that strong dependence on the laser polarization exists for the various two-photon vibrational transition lines. This dependence has not been previously observed for liquids, although such strong dependence on polarization for gases is well known (see Tam and Patel, 1979b, for details). However, as expected, the one-photon absorption line at 18 810 cm^{-1} is found to be independent of laser polarizations.

Our work in benzene demonstrates that multiphoton transitions in condensed matter can be readily observed by the pulsed OA technique. Multiphoton investigations are useful because they map out states that are not one-photon accessible (e.g., because of symmetry considerations). Furthermore, high-lying electronic states or ionization states can be reached by visible photons via multiphoton transitions. OA multiphoton spectroscopy should permit the discovery of many new multiphoton transitions (strong or weak) in condensed matter.

Earlier attempts at observation of two-photon absorption by optoacoustic methods (Bonch-Bruevich, Razumova, and Starobogatov, 1977) have shown that two-photon absorption cross sections for anthracene in alcohol at 6943 Å are $\approx 10^{-48}$ cm^4 sec $photon^{-1}$ $molecule^{-1}$, while those for POPOP solution at 6943 Å are $\approx 4 \times 10^{-48}$ cm^4 sec $photon^{-1}$ $molecule^{-1}$. Figure 30

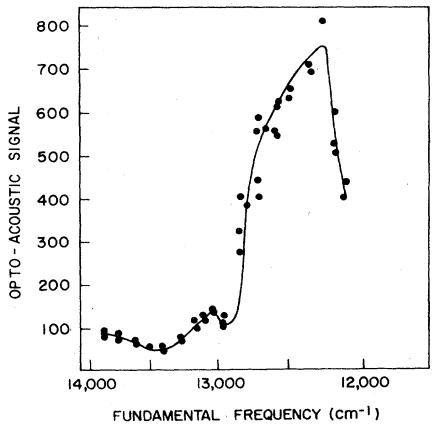

FIG. 30. Two-photon absorption spectrum of anthracene in alcohol measured by the pulsed laser optoacoustic technique. The two-photon absorption cross section at the peak is $\sim 10^{-48}$ cm^4 sec molecules^{-1} photon^{-1} (after Bonch-Bruevich *et al.*, 1977).

shows a two-photon absorption spectrum of anthracene measured with the optoacoustic technique. These data do not show the detailed vibronic structure we saw earlier for benzene, and further the peak two-photon absorption cross section of $\sim 10^{-48}$ cm^4 sec photon^{-1} molecule^{-1} suggests that the two-photon transition is a strongly allowed one, unlike the A_{1g}-B_{2u} transition of benzene, which shows a maximum two-photon absorption cross section of $\sim 10^{-51}$ cm^4 sec photon^{-1} molecule^{-1}. It is worth noting that the sensitivity of optoacoustic detection quoted by Bonch-Bruevich *et al.* (1977) is $\sim 10^{-6}$ J of absorbed single-pulse energy. This observation corresponds to three-to-four orders of magnitude lower sensitivity than that reported by Patel and Tam (1979a).

2. Raman-gain spectroscopy

There is strong current interest in Raman-gain spectroscopy (e.g., Heritage *et al.*, 1979; Levine and Bethea, 1979) because of its potentially high sensitivity in measuring Raman frequencies and cross sections, and because it is applicable to luminescent samples and hostile environments (flames, discharges, etc.), where spontaneous Raman scattering cannot be readily used.

The theory of Raman-gain spectroscopy is straightforward. A "pump" laser beam and a "signal" laser beam, of intensities I_p and I_s and frequencies ν_p and ν_s, respectively, are incident on a medium. The signal beam is defined to be the beam having the smaller frequency. If $\nu_p - \nu_s$ is equal to a Raman frequency ν_R of the medium, then Raman gain occurs, i.e., I_p is attenuated and I_s is amplified. We shall be concerned with small Raman gain only. In this case, we can show that the increase ΔI_s in the I_s passing through the medium is

$$\Delta I_s = g_s I_p I_s l \tag{56}$$

where l is the gain path length, and g_s is the Raman-gain coefficient (normalized to pump intensity) given by

$$g_s = \frac{16\pi^2 c^2 N(d\sigma/d\Omega)}{h\nu_s^3 n_s^2 (1+\bar{n})\Gamma} . \tag{57}$$

Here, c is the velocity of light, N is the scatterer density, $d\sigma/d\Omega$ is the differential Raman scattering cross section per scatterer, h is Planck's constant, n_s is the refractive index at ν_s, $1/(1+\bar{n})$ is the Boltzman factor for the ground state, and Γ is the spontaneous Raman scattering linewidth (full width at half maximum). In Eq. (56) we have assumed that the Raman gain g_s is small enough so that we can replace $e^{g_s I_p l}$ by $1 + g_s I_p l$. The conventional way to perform Raman-gain spectroscopy (Heritage *et al.*, 1979; Levine and Bethea, 1979) is to measure the incident I_s and the exit $(I_s + \Delta I_s)$. The difference between these two quantities is then evaluated to obtain ΔI_s. Since ΔI_s is usually small (e.g., much less than 10^{-3}), this method of subtracting one large number from another to get a small difference is possible only if each number can be very accurately measured; hence, stable and sophisticated laser sources are needed.

Our OA approach to this problem is to directly measure the difference. For each photon conversion from the pump beam to the signal beam, the amount of energy $h(\nu_p - \nu_s) = h\nu_R$ is lost from the optical beams and is deposited into the medium. Let the signal incident pulse energy be E_s and the increase in pulse energy be ΔE_s. Then the number of photons that have undergone conversion is $\Delta E_s/(h\nu_s)$. Hence the total energy deposited in the medium is

$$\Delta E_R = \Delta E_s(\nu_R/\nu_s) . \tag{58}$$

Integrating Eq. (56) over the duration of the laser pulses (the pump pulse and the signal pulse should occur over the same time interval), we have

$$\Delta E_s = g_s \bar{I}_p E_s l , \tag{59}$$

where $\bar{I}_p$ is an average pump intensity during a pulse. Combining Eqs. (58) and (59), we have

$$\Delta E_R = g_s l(\nu_R/\nu_s)\bar{I}_p E_s . \tag{60}$$

Equation (60) is the basis of OA Raman-gain spectroscopy (OARS). The energy ΔE_R that is deposited in the medium due to the Raman gain usually converts rapidly into heat in condensed media, and can be detected directly by the pulsed OA technique. Our work is the first demonstration of the use of OARS in liquids, although a similar technique in gases has recently been demonstrated by Barrett and Berry (1979).

A block diagram of the arrangement (Patel and Tam, 1979c) for OARS in liquids is shown in Fig. 31. In this setup, two flash-lamp-pumped dye lasers are synchronized. Laser I uses Coumarin 504 dye, while Laser II uses Rhodamine 6G dye. Both operate at 10 pulses per second. The two laser beams are combined by a dichroic mirror, and focused into the center of the OA cell. The red frequency ν_s is fixed, while the green frequency ν_p is scanned. When the Raman resonance condition, $\nu_p = \nu_s + \nu_R$, is satisfied for ν_R equal to the Raman excitation frequency of the medium, the OA signal is detected by the piezoelectric transducer. The pulse energy of Laser I varies over its scanning range. Hence the OA signal is normalized to the pulse energy of Laser I to give a normalized OARS signal $S(\nu_R)$. Here ν_R is defined as $\nu_p - \nu_s$. $S(\nu_R)$ is thus directly proportional to the Raman cross section

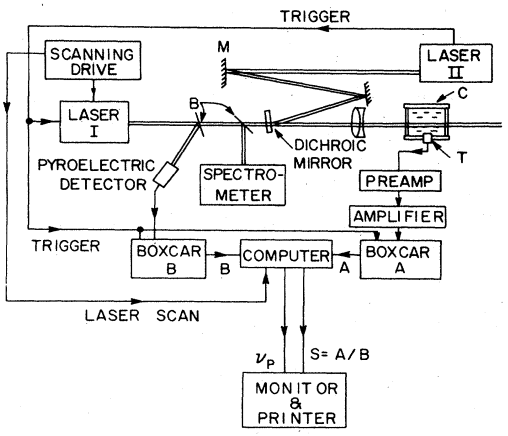

FIG. 31. Experimental arrangement for OARS, C=cell, T =transducer, M=beam-steering mirrors, and B=5% reflectivity beam-splitting. Laser I is the pump laser operating with Coumarin 504 dye, while Laser II is the signal laser with Rhodamine 6G dye.

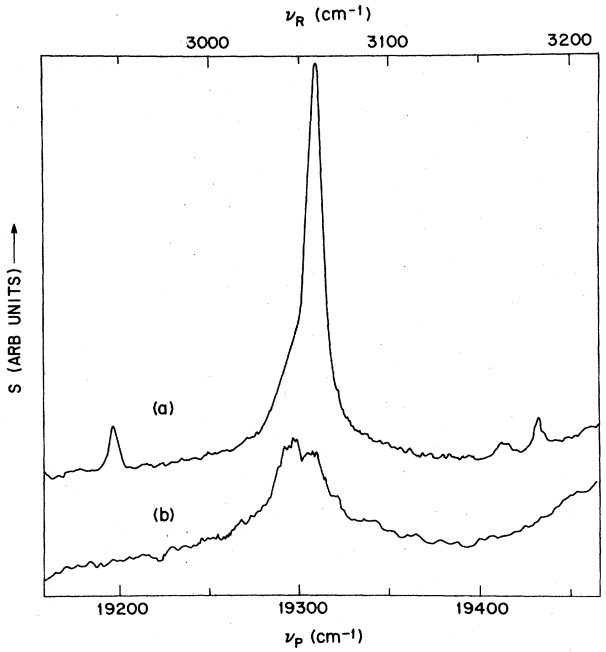

FIG. 32. Optoacoustic Raman-gain spectra of benzene for (a) parallel and (b) orthogonal pump and signal polarizations.

$d\sigma/d\Omega$, as seen from Eqs. (60) and (57). Since ν_s is not scanned, its pulse energy E_s should ideally remain constant during the experimental scan (typically taking several minutes), for a stable enough laser. In our case, E_s actually fluctuates by ±10% during the scan. This constitutes a major source of noise in our OARS studies so far. This source of noise could be eliminated either by having a much more stable Laser II, or by further normalizing $S(\nu_R)$ by E_s (measured by another detector). Another important source of noise in our OARS investigations is the relative time jitter of the two laser pulses; the jitter is as large as ±30% of the laser pulse width of ~1 μsec. Ideally, the two laser sources for OARS should be automatically synchronized. This could be done by using a two-color flash-lamp-pumped dye laser (one flash-lamp pumping two dye cells simultaneously). Alternately, a laser-pumped dye laser could be used, and part of the pumping laser split off and combined with the dye laser to perform OARS.

Some examples of OARS data for various liquids are shown in Figs. 32 and 33. These data have been obtained with the nonideal arrangement shown in Fig. 31, and significant improvements in signal-to-noise should be possible with better laser sources as discussed above. We further note that the data of Fig. 32(a) are obtained with the two laser polarizations parallel; hence $S(\nu_R)$ is proportional to the polarized Raman cross section. Totally different spectra have been obtained (Patel and Tam, 1979c) with the two laser polarizations orthogonal, as seen in Fig. 32(b), in which case $S(\nu_R)$ is proportional to the depolarized Raman cross section. Further (Patel and Tam, 1979c), we have shown a capability of measuring Raman gain as small as 10^{-5} cm^{-1} using the OARS technique. The data reported in Fig. 33 were obtained for the case of parallel polarizations.

Additional desirable features of OARS include the following. Since pulsed lasers are used, transient OARS due to decaying species can be readily studied in a time-resolved experiment. Background luminescence poses no serious problem for the use of OARS. For cases where the Raman-excited vibrational modes decay slowly (e.g., in liquid N_2), collisional quenching can be investigated by systematically adding foreign molecules to the liquid and studying the increase in the OARS signal. Furthermore, the experimental apparatus needed for OARS is simple (much less sophisticated than that needed for conventional Raman-gain measurements). Thus OARS should be extremely useful for

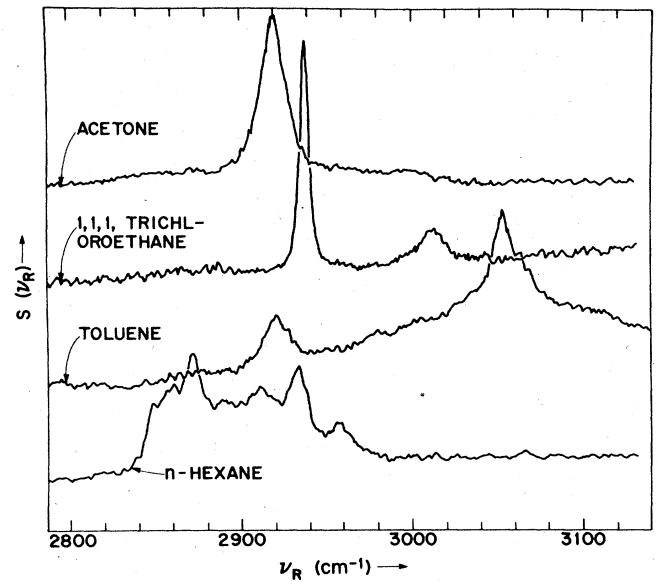

FIG. 33. Examples of OARS signal observed for various liquids. Laser polarizations are parallel for these signals.

liquids, including aqueous solutions and biological samples.

Nechaev and Ponomarev (1975) have proposed the use of an optoacoustic measurement technique for Raman spectroscopy of gaseous media. The scheme described is similar to the one used in the study of OARS spectra of liquids described here, but utilizes cw lasers for the study of low-pressure gases, and microphones for detection of optoacoustic signals. Barrett and Berry, 1979, have recently demonstrated the effectiveness of this technique for the study of Raman spectra of gases.

VI. OTHER OA SPECTROSCOPY STUDIES

A. OA spectroscopy and luminescence spectroscopy

The use of optoacoustic spectroscopy as a supplement to luminescence spectroscopy in the study of energy relaxation and energy-transfer processes in condensed media is exciting, since now we can take into account both the radiative and the nonradiative relaxation processes. Razumova and Starobogatov (1977) have described some preliminary experimental and theoretical studies using optoacoustic spectroscopy and luminescence spectroscopy for the quenching "down" and quenching "up" of excited states in fluorescent organic solutions. They employed a pulsed ruby (including frequency doubled radiation) laser. They measured the optoacoustic signal (derived from an immersed piezoelectric transducer) as a function of the luminescence signal in a three-level system, where level one is the ground state, level two is the first excited state (from which luminescence can originate), and level three is another excited state to which quenching transitions are made through absorption of radiation, corresponding to the transition between states two and three. The detailed theoretical description of rate equations governing the luminescence and optoacoustic signal output (for an assumed model) was in good agreement with measured variation of the optoacoustic signal and the luminescence signals as the pumping radiation and the quenching radiation intensities were changed. It is clear that studies such as these where, in addition to the intensities, the frequencies of the two radiation sources are varied [not done in the Razumova and Starobagotov (1977) studies] will provide significant information regarding redistribution of excitation within a system following excitation. Further, use of picosecond pulse lasers and time gating of the excitation and quenching pulses (whether nanosecond or picosecond duration) will provide additional information on the kinetics of excitation redistribution. As an extension of this technique, Starobogatov (1977) has used the measured optoacoustic signal as a means of determining luminescence efficiency of dye solutions. This is straightforward, since the absorbed energy (from the exciting beam) and energy released through nonradiative processes (measured as the optoacoustic signal) are measured in the experiment, and thus the total luminescence output is the difference between these two numbers. The advantage of this scheme over the traditional optical measurement method is that there is no need to introduce corrections for the spectral sensitivity of the photodetector and locations and shapes of the luminescence spectra of the sample and a standard.

B. Pulsed OA spectroscopy in strongly absorbing liquids

Our primary interest is in the area of optoacoustic spectroscopy of very low-loss materials. But experimental studies of Sigrist and Kneubuhl (1978), in which they have investigated optoacoustic signal generation in strongly absorbing liquids using a pulsed CO_2 laser as the source ($\alpha \approx 1-1000\ cm^{-1}$), provide some data to support the theoretical considerations above. In the strongly absorbing case, we are dealing not with cylindrical, but with hemispherical geometry in the generation of an OA signal. However, some comparisons should be possible. In particular, the optoacoustic pulse shape which is predicted to consist of a positive and a negative pulse separated by time of the order of the duration of the laser pulse appears to have been verified. In Fig. 34 we show the stress transient in water for CO_2 laser pulse energies below vaporization threshold, as observed by Sigrist and Kneubuhl. In agreement with the predictions of Eq. (38), the optoacoustic signal consists of a compressional pulse followed by an almost equal rarefaction pulse. (Detailed theoretical arguments and computer solution of the sound generation equation by Sigrist and Kneubuhl are also able to reproduce the experimentally observed pulse shapes.) It should be emphasized, however, that because the authors have investigated only highly absorbing liquids at CO_2 laser wavelengths, it is possible to deposit enough energy to vaporize the liquid. In this situation, considerably different pulse shapes are observed.

C. Other phenomena at high intensities

At very high laser intensities, it is possible to be confronted with breakdown and bubble formation in liquids. For example, when the nonradiatively released energy in water exceeds $\sim 2240\ J\,cm^{-3}$, there is a possibility of vapor bubble formation. Since breakdown and associated explosive nonradiative relaxation results in acoustic pulse generation, the optoacoustic detection scheme can be utilized for gaining insights into these phenomena. Teslenko (1977) has reported a

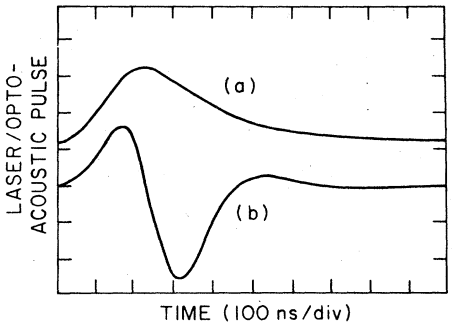

FIG. 34. Optoacoustic signal generated in water due to absorption of a pulse of CO_2 laser radiation. Top: Laser pulse. Bottom: Optoacoustic signal showing the compressional and the rarefaction pulses (after Sigrist and Kneubühl, 1978).

study of the optoacoustic and optohydrodynamic parameters of laser breakdown in water, glycerine, and benzene, using a 1 J, 10–70 nsec duration ruby laser. For measurements of linear or nonlinear optical absorption using the optoacoustic technique under discussion in this review, it is very unlikely that the absorbed energy will approach a value anywhere close to that necessary for shock wave and cavity formation.

D. cw-source-based OA spectroscopy with piezoelectric transducer

One of the earliest demonstrations of the use of a piezoelectric transducer (either immersed in a liquid or attached to a solid) for measurements of optical absorption was that of Kohanzadeh *et al.* (1975). These authors used a cw argon ion laser at either 4880 Å or 5145 Å (1.5 W), a hollow cylindrical PZT transducer which was filled with the liquid under investigation, and a mechanical chopper or an electro-optic modulator (which gave a sinusoidal modulation). Since the wavelength of the laser was fixed, no spectroscopy was carried out, but some of the features of immersed-transducer optoacoustic spectroscopy were recognized. These included a linear dependence of the optoacoustic signal on input power and absorption coefficient (varied by use of methylene blue dye added to control the absorption), and the time delay of the acoustic signal measured by determining the phase delay detected with a lock-in amplifier. These authors further recognized the important resonant response behavior of the piezoelectric transducer for optoacoustic spectroscopy. They used a cylindrical piezoelectric ceramic that was simultaneously the container for their liquids and the detector for acoustic signals, as shown in Fig. 35. The optoacoustic voltage output from their cylindrical transducer is plotted as a function of the laser modulation frequency in Fig. 36. The absorption of the liquid (acetone) was increased by the addition of a dye. The range of absorption coefficients investigated was 0.005 to 0.5 cm^{-1}; however, the lower values of the absorption coefficient were measured not with the optoacoustic technique but with a thermal lens technique (Hu, 1973). Although no attempt was made to extend the technique

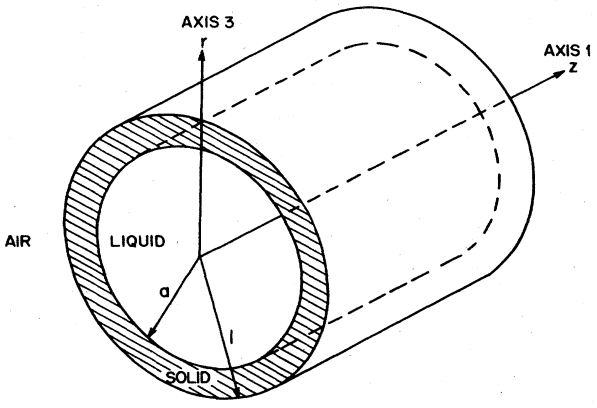

FIG. 35. Optoacoustic cell consisting of a piezoelectric material cylinder that doubles as the container for the liquid being studied (after Kohanzadeh *et al.*, 1975).

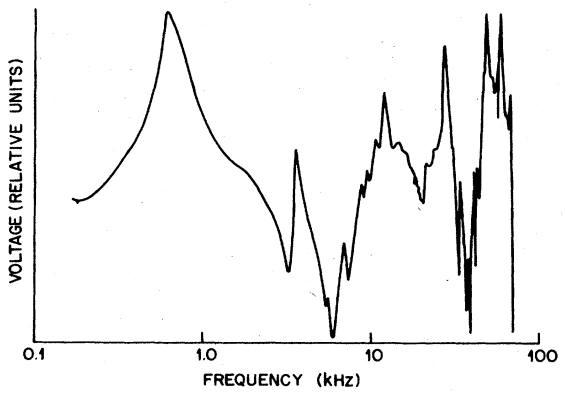

FIG. 36. Optoacoustic signal as a function of laser modulation frequency (for the case of a cylindrical transducer-container geometry shown in Fig. 35), showing the effect of transducer and other resonances (after Kohanzadeh *et al.*, 1975).

of using a cw source, piezoelectric detector, and lock-in amplifier to measurement of small absorption coefficients, it is clear that at the cw power level of 1.5 W, even the lower limit of 0.005 cm^{-1} was beyond the capabilities of the technique. The limitations of the method stemmed mainly from adherence to a cw source. It can be shown that with the same average power of 1.5 W, but in the form of pulses of ~1–2 μsec duration and 10–15 pulses per second (pps) repetition rate, sensitivity could have been much improved. In other words, if we take the sensitivity achieved by Patel and Tam (1979b) to be ~10^{-6}–10^{-7} cm^{-1} using input pulse energies of 1 mJ and peak powers of ~1 kW with a pulse repetition frequency of ~10 pps, we can extrapolate to the case of 1.5 W peak power, pulse repetition frequency of ~100 kHz (square wave modulation). We find the extrapolated sensitivity for the Kohanzadeh experiments to be

$$\alpha_{\min}(K)=\alpha_{\min}(PT)\left(\frac{P_K}{P_{PT}}\right)\left(\frac{f_{PT}}{f_K}\right)^{1/2}, \tag{61}$$

where P_K and P_{PT} are peak laser powers, f_K, f_{PT} are pulse repetition frequencies, and $\alpha_{\min}(K)$ and $\alpha_{\min}(PT)$ are the minimum detectable absorption coefficients for the Kohenzadeh and Patel-Tam experiments, respectively. With $\alpha_{\min}(PT)=10^{-7}$ cm^{-1}, $P_K=1.5$ W, $P_{PT}=10^3$ W, $f_{PT}=10$ Hz, and $f_K=10^5$ Hz,

$$\alpha_{\min}(K)=10^{-7}\left(\frac{10^3}{1.5}\right)\left(\frac{10}{10^5}\right)^{1/2}$$
$$=7\times10^{-7}\ cm^{-1}. \tag{62}$$

The discrepancy, then, between the observed and the calculated sensitivities is puzzling.

In a subsequent paper, Farrow *et al.* (1978), recognizing the importance of acoustic impedance matching for optimum detection of the optoacoustic signal carried further the earlier studies of Kohanzadeh *et al.* (1975), still using cw argon ion lasers or dye lasers, and either mechanically chopping or electro-optically modulating the laser output (see Fig. 37). While they clearly appreciated the versatility of the piezoelectric transducers over the gas-phase microphone photoacoustic spectroscopy technique of Harshbarger and Robin

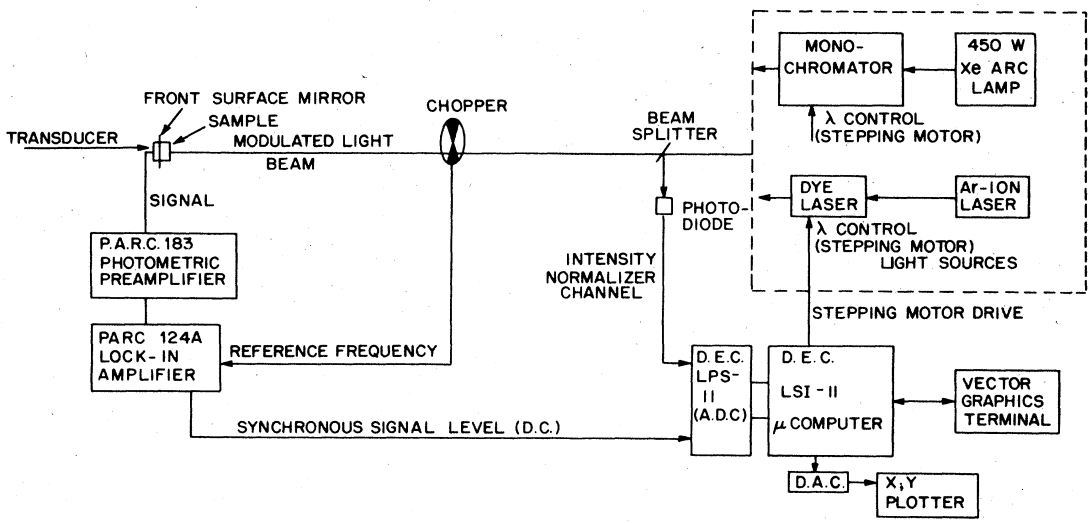

FIG. 37. Experimental setup for optoacoustic spectroscopy with attached transducer, using chopped or electro-optically modulated laser radiation in radiation derived from a xenon arc-lamp–monochromator combination (after Farrow *et al.*, 1978).

(1973), and Rosencwaig (1973), their conclusion was that the sensitivity achieved with the piezoelectric transducer scheme was similar to that achieved with gas-phase photoacoustic spectroscopy. Thus it is apparent from their published data that Farrow *et al.* (1978) failed to achieve the ultra-low-absorption-coefficient measurement capability afforded by the pulsed laser, immersed or attached piezoelectric transducer, gated detection technique that is the central subject of the present review.

An extensive study of the cw-laser-based optoacoustic technique utilizing an attached piezoelectric transducer has been carried out by Hordvik and his collaborators and reported in a number of elegant papers (Hordvik, 1977; Hordvik and Schlossberg, 1977; Hordvik and Skolnik, 1977). In their study of low-loss optical solids Hordvik and Schlossberg (1977) used cw CO, CO_2, or argon ion lasers with a piezoelectric transducer attached directly to the sample of optical material. Recognizing the importance of false optoacoustic signals that may arise due to scattered light from the bulk of the optical material being absorbed by the attached piezoelectric transducer, they placed a second transducer symmetrically with respect to the optical beam, close to but not in acoustical contact with the sample (see Fig. 38). They argued that by subtracting the unattached-transducer signal from the attached-transducer signal, the effect of bulk scattered light, especially in low-absorption-loss materials, could be minimized. Further, by the proper choice of sign and magnitude of the piezoelectric constant of the transducer material, the optoacoustic signal generated by bulk absorption could be made to be exactly 180° out of phase with that generated due to surface absorption. They also observed that the dependence of the optoacoustic voltage output on the distance between the transducer and the laser-illuminated region is different for signals arising from bulk and surface absorption losses. Thus it is possible to separate out the two quantities from measured data. Hordvik and Skolnik (1977) estimate that surface and bulk absorption losses in the 10^{-5} cm^{-1} range can be determined with cw laser powers of the order of *a few hundred milliwatts* and that the limitation to the sensitivity arises from false signals generated by scattered radiation reaching the transducer. Because of the low-frequency chopping rates involved in these studies, Skolnik and his collaborators were not able to use the time of flight or special geometrical schemes described in Secs. V.A.3 and V.A.4 which contribute significantly to the reduction and/or elimination of false signals arising from scattering when using the pulsed laser, immersed or attached piezoelectric transducer, and gated detection. However, for good single crystal materials such as CaF_2, SrF_2, BaF_2, MgO, Al_2O_3, LiF, etc., the cw laser scheme of Skolnik and colleagues has allowed them to measure bulk absorption coefficients as low as 10^{-4} cm^{-1} as seen from the data for BaF_2, SrF_2, and CaF_2 in Fig. 39.

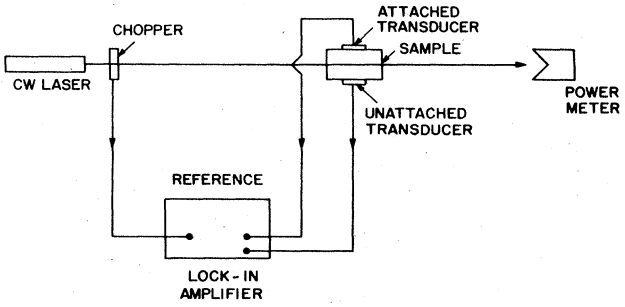

FIG. 38. Attached-transducer optoacoustic technique for subtracting out scattered light signals for measurements of low-optical-loss solids using chopped cw lasers as sources (after Hordvik, 1977).

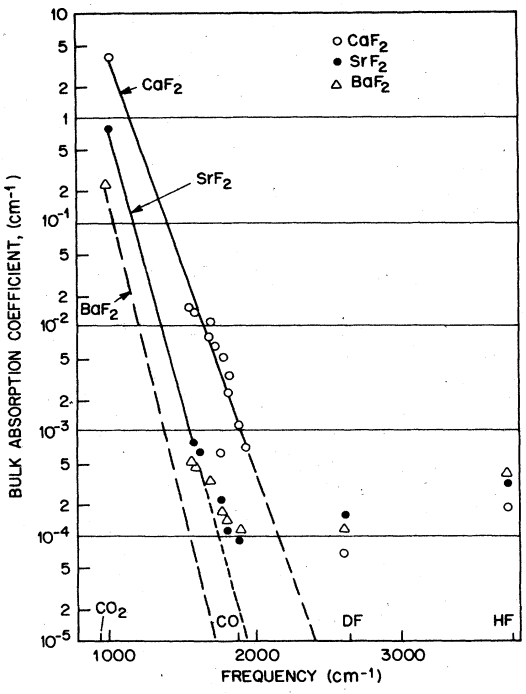

FIG. 39. Infrared absorption spectra of BaF_2, SrF_2, and CaF_2 obtained using attached-transducer, cw laser (chopped) technique. Lasers used for these measurements include various fixed-frequency transitions from the CO_2, CO, DF, and HF lasers (after Hordvik, 1977).

E. Application of OA spectroscopy to trace detection in liquids

The ability of optoacoustic spectroscopy to measure ultra-small absorption coefficients in gases (Patel and Kerl, 1977; Kreuzer and Patel, 1971) has found extensive applications in the area of trace gas detection, i.e., pollutant measurements (see, for example, Patel, 1978, and Pao, 1977). For liquids we have seen that absorption coefficients as small as 10^{-7} cm^{-1} can be measured using the pulsed laser, immersed transducer, and gated detection. Applications of the technique to trace detection in liquids have been reported very recently by Voigtman *et al.* (1981). There have also been reports of the use of cw-laser-based techniques, with piezoelectric transducers for such measurements with varying degrees of success. Lahmann *et al.* (1977) used the cw-laser technique first described by Kohanzadeh *et al.* (1975) in essentially unchanged form. They determined trace β carotene in chloroform using the 5145 Å transition of the argon ion laser as a source of radiation, and established a detection limit of 9×10^{10} molecules cm^{-3} [12 parts per trillion (ppt)]. Oda *et al.* (1978) applied essentially the same technique to the detection of trace cadmium in penicillin ochro-chloron after its decomposition and extraction into chloroform. Using ~500 mW of argon ion laser power at 5145 Å, and a chopping frequency of 185 Hz, a detection limit of 0.02 ng ml^{-1} was deduced for cadmium (14 ppt). It is worth noting here that for reproducible detection of trace elements in liquids, using the Lahmann *et al.* or Oda *et al.* schemes, eventually use will have to be made of cw tunable dye lasers of sufficient power output as sources; these are both more difficult and more expensive to build than pulsed dye lasers of the type used in the present review. The need for tunable rather than fixed lasers arises from practical situations in which more than one trace element is present, with partially overlapping absorption features.

The pulsed laser scheme, using an immersed transducer and gated detection, is able to measure absorption coefficients of ~10^{-7} cm^{-1}. From this detection capability we can estimate the trace constituent concentration that can be measured. For a trace constituent peak absorption coefficient of ~10^{4}–10^{5} cm^{-1}, we extrapolate to a detection capability of ~1–10 ppt, assuming the background absorption of the solvent is smaller than ~10^{-7} cm^{-1}. This last requirement places rather stringent limits on the detectability of trace constituents, since we have seen that for pure water the smallest optical absorption coefficient in the visible region is ~2×10^{-4} cm^{-1}. Thus the use of optoacoustic spectroscopy for trace detection in water will be limited to ~100 ppt unless the trace constituent has sharp absorption features and/or the trace constituent can be extracted into another liquid such as CCl_4 that has a very low absorption coefficient in the visible region.

VII. DISCUSSIONS

A. Summary of present status

We now summarize the advantages of our pulsed OA spectroscopy technique, as compared to the conventional OA technique using chopped cw laser beams, gas-phase microphones, and lock-in detections. These advantages are

(a) High detection sensitivity. We can presently detect absorbed energy of ~10^{-10} J, in a 1 cm path length. For a laser pulsed energy of 1 mJ, this corresponds to a detection limit of ~10^{-7} cm^{-1} for absorption coefficient. Further improvements are possible, as discussed earlier.

(b) The use of a pulsed laser, with its high peak power (~kW), permits the ready OA detection of nonlinear absorption, like multiphoton absorption or stimulated Raman scattering. However, the duty cycle of the laser is very low, so that the average power is small (~10 mW). Hence spurious effects due to heating of the liquid and convection currents are avoided.

(c) The technique of time gating, possible only with pulsed OA detection, is a very useful method for discriminating against spurious OA signals like those due to light scattering or window absorptions.

(d) High-resolution studies are possible by narrow-banding the laser with intracavity etalons.

(e) Absolute calibration for liquids is readily obtained.

(f) There is no complex dependence of the OA signal on thermal diffusion length, on chopping frequency, etc., as in the conventional method (Rosencwaig, 1973; Rosencwaig and Gersho, 1976; Rosencwaig, 1977; Rosencwaig, 1978).

We note that high sensitivity is the major advantage of the pulsed laser OA technique using immersed or

attached piezoelectric transducer and gated detection. High sensitivity results from high signal strength and/or low noise. A strong signal is possible in our case because of the use of PZT transducers in direct contact with the liquid or solid studied. The good acoustic impedance matching and fast rise time of the transducer result in a high signal level. Furthermore, negligible thermal diffusion takes place during the laser pulse, so maximum expansion of the irradiated sample occurs. Low noise is possible because we are detecting high-frequency ultrasonic waves, so that bandpass filters (transmitting 100–500 kHz) can be used in the preamplifier circuit. This is a great advantage, since the laboratory environment is very noisy at low frequencies (dc-10 kHz), owing to mechanical vibrations, multiples of line frequencies, etc. The use of time gating is crucially important in reducing the noise. Furthermore, the low light-scattering geometry and high polish of the inner surface of the cell also minimize noise due to light scattering.

B. Examples of further experiments

The advantages of the pulsed OA technique, which include high sensitivity, high noise discrimination, and applicability to linear and nonlinear spectroscopy, can clearly be exploited in many possible future investigations or applications, and we enumerate a few below.

a. Low-temperature OA *spectroscopy.* Optical absorption features in high-pressure gases at low temperature have been of special interest to the astrophysics community for the elucidation of the composition of the atmospheres of planets such as Jupiter, Saturn, and Uranus. For example, collision-induced overtone absorptions in hydrogen have been identified in the above planetary spectra. But for the third and higher overtones in hydrogen, no laboratory data exist, since very long path lengths, low temperatures, and high pressures are needed for the measurement of weak absorptions using conventional techniques. The OA spectroscopic technique described in the present paper is ideally suited for making many of the desired measurements. Further, by going to yet lower temperatures, optical absorption features in simple cryogenic fluids (such as H_2, HD, O_2, N_2, CH_4) arising from the overtone absorptions can be studied. Collisional nonradiative decays of metastable vibrationally excited homonuclear diatomic molecules in cryogenic liquids can be readily studied over a wide temperature range. In addition, OA spectra of solids, powders, and films can now be readily obtained over a wide range of temperatures.

b. Higher-order Raman processes. The ability of OARS to measure Raman gains as small as 10^{-5} cm^{-1}, even today, points to a direct application of the OARS to the study of higher-order Raman processes which have smaller Raman scattering cross sections than those presently studied. A specific example is hyper-Raman scattering, which is at present considered a very difficult experimental subject. A preliminary estimate indicates that OARS could make these measurements easier in many situations.

c. Materials testing. Materials for low-attenuation applications (e.g., for optical fibers or for laser windows) can be tested.

d. Trace detection. Minute quantities of foreign molecules in a liquid or solid can be detected by choosing a laser frequency that is absorbed strongly only by the molecules of interest. Alternately, OARS can also be used to map out the vibrational frequencies of the foreign molecules.

e. Forbidden transitions. Many transitions that are "forbidden" (e.g., symmetry-forbidden transitions or singlet-triplet transitions) are actually weakly allowed due to various perturbations, or they can be made allowed by externally applied fields. Our high-sensitivity technique will allow the observation of many forbidden transitions.

f. Excited states. OA spectra and lifetimes of excited states can be readily obtained by the pulsed OA technique, with variable time delay of the laser OA pulses after the production of the excited species. (This, however, requires the use of nonresonant transducers.)

g. Monolayers. Electronic absorption spectra and Raman spectra of monolayers are subjects of strong current interest for our understanding of the structure of monolayers and surfaces. The pulsed OA method (linear absorption or OARS) seems quite adaptable for these studies. OA two-photon spectroscopy of monolayers should also be a new and interesting area of research.

h. OA *microscopy.* Another field of strong interest is OA imaging and microscopy (Busse, 1979; Pouch *et al.*, 1979; Wong *et al.*, 1978) because of its important possible applications in science and technology. Both thick samples and thin-sliced samples could be studied by our pulsed OA technique. OA microscopy done with different laser frequencies should provide valuable information, e.g., in diagnostics of integrated circuit wafers or in studying biological samples.

i. Other excitation sources. We have, in this review, discussed only optical sources (tunable lasers, fixed-frequency lasers, etc.) for providing excitation through the absorption of the radiation. The technique of acoustic detection of absorbed energy (especially when the absorbed energy is released from the medium through nonradiative mechanisms) is a general one and is independent of the specifics of the source of excitation. Thus it should be possible to carry out electron energy-loss spectroscopy as well as x-ray absorption spectroscopy using the submerged (for a liquid) or attached (for a solid) piezoelectric transducer technique in a manner similar to that described in this review. In particular, availability of pulsed monoenergetic electron beams and pulsed x-ray sources such as the synchrotron radiation sources should make the transition from optoacoustic spectroscopy to electron energy-loss acoustic spectroscopy and x-ray absorption acoustic spectroscopy possible in the near future.

C. Other OA methods

In this article, we have been mainly concerned with the theory and applications of the pulsed OA spectroscopy method, for which many novel and quantitative

uses have been demonstrated, and will be possible; we hope that this review will be helpful for researchers planning to use this simple but useful technique.

However, we do not mean to imply that conventional optoacoustic techniques or photoacoustic techniques, as they are often called (e.g., Harschbarger and Robin, 1973; Rosencwaig, 1973, 1976, 1977, 1978) are not useful. They have sensitivities a few orders of magnitude less than that demonstrated using the pulsed laser technique, with immersed (in the case of a liquid) or attached (in the case of a solid) transducer and gated detection. Thus if high sensitivity is desired, the pulsed optoacoustic technique is definitely indicated. However, in studies where only low sensitivities are required, (e.g., in totally opaque samples), the conventional gas-phase microphone (i.e., solid-gas-microphone) method can be used. Indeed, applications like depth-profiling of totally opaque samples by varying the chopping frequency of the cw light beam can only be performed with the conventional method. In view of the usefulness of the conventional OA technique in certain applications, and the fast growth of interest in OA measurements in condensed matter, we have collected a list of recent relevant papers, as outlined in the Appendix. No claim can be made for completeness in this list, but we hope that it will provide a helpful guide to current research interests.

ACKNOWLEDGMENTS

We should like to thank R. J. Kerl for his assistance in the construction of the OA cells and preamplifiers. We also thank V. E. Bondybey, T. D. Harris, S. Geschwind, E. I. Gordon, R. A. Lemons, S. L. McCall, G. L. Miller, P. M. Rentzepis, M. B. Robin, J. Stone, M. D. Sturge, and B. A. Wilson, for their useful suggestions, enlightening comments, and fruitful discussions at various stages of this work.

APPENDIX: RECENT WORK IN THE OA STUDY OF CONDENSED MATTER

Subject	References
1. Conventional OA cell	
a. Experiment	Blank and Wakefield, 1979 Cahen and Garty, 1979 Callis *et al.*, 1969 Callis, 1976 Eaton and Stuart, 1978 Gray *et al.*, 1977 Kanstad and Nordal, 1978 McClelland and Kniseley, 1976 McDavid *et al.*, 1978 Monahan and Nolle, 1977 Nordal and Kanstad, 1977 Quimby *et al.*, 1977 Rosencwaig, 1973 Rosencwaig, 1977 Shaw, 1979 Tam and Wong, 1980
b. Theory	Aamodt *et al.*, 1977 Aamodt and Murphy, 1978 Bennett and Forman, 1977 McDonald and Wetsel, Jr., 1978 Rosencwaig and Gersho, 1976
2. Applications of OA spectroscopy	
a. Quantum yields	Adams *et al.*, 1977 Lahmann and Ludewig, 1977 Merkle and Powell, 1977 Murphy and Aamodt, 1977 Quimby and Yen, 1978 Razumova and Starobogatov, 1977 Rockley and Waugh, 1978 Starobogatov, 1977
b. Surface absorptions	Adams *et al.*, 1978 Hordvik and Skolnik, 1977 Kerr, 1973 Parker, 1973 Patel and Tam, 1980

Subject	References
c. Trace analysis	Lahmann *et al.*, 1977 Oda *et al.*, 1978
d. Absolute absorption coefficient	Patel and Tam, 1979b Patel *et al.*, 1979 Patel and Tam, 1979d Tam *et al.*, 1979 Tam and Patel, 1979b Wetsel, Jr., and McDonald, 1977
e. Dichroism	Fournier *et al.*, 1978 Palmer *et al.*, to be published
f. Others	Cahen, 1978 Gray and Bard, 1978 Robin and Kuebler, 1977 Tam and Patel, 1979c
3. Optoacoustic generation	
a. Strong absorption, surface heating	Askaryan *et al.*, 1963 Bell and Landt, 1967 Bonch-Bruevich *et al.*, 1975 Bushanam and Barnes, 1975 Emmony *et al.*, 1976 Gordienko *et al.*, 1978 Gournay, 1966 Von Gutfeld and Budd, 1979 Sigrist and Kneubühl, 1978 Sladky *et al.*, 1977 Teslenko, 1977 White, 1963
b. Weak, bulk absorption	Bonch-Bruevich, 1977 Bunkin and Komissarov, 1973 Egerev and Naugol'nykh, 1977 Farrow *et al.*, 1978 Gorodetskii *et al.*, 1978 Kasoev and Lyamshev, 1977 Lyamshev and Naugol'nykh, 1976 Naugol'nykh, 1977 Westervelt and Larson, 1973
c. Electrostriction	Bebchuk *et al.*, 1978 Brueck *et al.*, 1980
4. Piezoelectric OA detection	Burt, 1979 Farrow *et al.*, 1978 Hordvik and Schlossberg, 1977 Kohanzadeh *et al.*, 1975 Patel and Tam, 1979a Rentzepis and Pao, 1966 Rosencwaig *et al.*, 1979 Wetsel and McDonald, 1979
5. OA microscopy	Busse, 1979 Pouch *et al.*, 1979 Wang *et al.*, 1979 Wickramasinghe *et al.*, 1978 Wong *et al.*, 1978
6. OA detection of nonlinear absorptions	Bonch-Bruevich *et al.*, 1977 Cox, 1978 Patel and Tam, 1979c Rentzepis and Pao, 1966

Subject	References
7. Reviews	Rockley and Devlin, 1977 Tam and Patel, 1979a Harshbarger and Robin, 1973 Hordvik, 1977 Pao, 1977 Robin, 1976 Rosencwaig, 1978 Somoano, 1978

REFERENCES

Aamodt, L. C., J. C. Murphy, and J. G. Parker, 1977, J. Appl. Phys. **48**, 927.

Aamodt, L. C., and J. C. Murphy, 1977, J. Appl. Phys. **48**, 3502.

Aamodt, L. C., and J. C. Murphy, 1978, J. Appl. Phys. **49**, 3036.

Adams, M. J., B. C. Beadle, G. F. Kirkbright, and K. R. Menon, 1978, Appl. Spectrosc. **32**, 430.

Adams, M. J., J. G. Highfield, and G. F. Kirkbright, 1977, Anal. Chem. **49**, 1850.

Askaryan, G. A., A. M. Prokhorov, G. F. Chanturiya, and G. P. Shipulo, 1963, Zh. Eksp. Teor. Fiz. **44**, 2180 (Sov. Phys.—JETP **17**, 1463).

Barrett, J. J., and M. J. Berry, 1979, Appl. Phys. Lett. **34**, 144.

Bebchuk, A. S., V. M. Mizin, and N. Ya Salova, 1978, Opt. Spektrosk. **44**, 158 [Opt. Spectrosc. (USSR) **44**, 92].

Bell, C. E., and J. A. Landt, 1967, Appl. Phys. Lett. **10**, 46.

Bennett, H. S., and R. A. Forman, 1977, Appl. Opt. **16**, 2834.

Blank, R. E., and T. Wakefield II, 1979, Anal. Chem. **51**, 50.

Bonch-Bruevich, A. M., T. K. Razumova, and I. O. Starobogatov, 1975, Pis'ma Zh. Tech. Fiz. **1**, 65 (Sov. Phys.—Tech. Phys. Lett. **1**, 26).

Bonch-Bruevich, A. M., T. K. Razumova, and I. O. Starobogatov, 1977, Opt. Spektrosk. **42**, 82 [Opt. Spectrosc. (USSR) **42**, 45].

Brilmyer, G. H., A. Fujishima, K. S. V. Santhanam, and A. J. Bard, 1977, Anal. Chem. **49**, 2057.

Brueck, S. R. J., H. Kildal, and L. J. Belanger, 1980, Opt. Commun. **34**, 199.

Bunkin, F. V., and V. M. Komissarov, 1973, Akust. Zh. **19**, 305 (Sov. Phys.—Acoust. **19**, 203).

Burt, J. A., 1979, J. Acoust. Soc. Am. **65**, 1164.

Bushanam, G. S., and F. S. Barnes, 1975, J. Appl. Phys. **46**, 2074.

Busse, G., 1979, in Technical Digest, Topical meeting in photoacoustic spectroscopy, Ames, Iowa (unpublished).

Cahen, D., 1978, Appl. Phys. Lett. **33**, 810.

Cahen, D., and H. Garty, 1979, Anal. Chem. **51**, 1865.

Callis, J. B., 1976, J. Res., Nat. Bur. Stand. **80A**, 413.

Callis, J. B., M. Gouterman, and J. D. S. Danielson, 1969, Rev. Sci. Instrum. **40**, 1599.

Cox, D. M., 1978, Opt. Commun. **24**, 336.

Eaton, H. E., and J. D. Stuart, 1978, Anal. Chem. **50**, 587.

Egerev, S. V., and K. A. Naugol'nykh, 1977, Akust. Zh. **23**, 738 (Sov. Phys.—Acoust. **23**, 422).

Emmony, D. C., M. Siegrist, and F. K. Kneubühl, 1976, Appl. Phys. Lett. **29**, 547.

Farrow, M. M., R. K. Burnham, M. Auzanneau, S. L. Olsen, N. Purdie, and E. M. Eyring, 1978, Appl. Opt. **17**, 1093.

Fournier, D., A. C. Boccara, and J. Badoz, 1978, Appl. Phys. Lett. **32**, 640.

Gordienko, V. M., A. B. Reshilov, and V. I. Shmal'gauzen, 1978, Akust. Zh. **24**, 132 (Sov. Phys.—Acoust. **24**, 73).

Gorodetskii, V. S., S. V. Egerev, I. B. Esipov, and K. A. Naugol'nykh, 1978, Kvant. Elektron (Moscow) **5**, 2396 (Sov. J. Quantum Electron. **8**, 1345).

Gournay, L. S., 1966, J. Acoust. Soc. Am. **40**, 1322.

Gray, R. C., and A. J. Bard, 1978, Anal. Chem. **50**, 1262.

Gray, R. C., V. A. Fishman, and A. J. Bard, 1977, Anal. Chem. **49**, 697.

Gruber, J. B., J. R. Henderson, M. Muramoto, K. Rajnak, and J. G. Conway, 1966, J. Chem. Phys. **45**, 477.

Hale, G. M., and M. R. Querry, 1973, Appl. Opt. **12**, 555.

Harshbarger, W. R., and M. B. Robin, 1973, Acc. Chem. Res. **6**, 329.

Hass, M., and J. W. Davisson, 1977, J. Opt. Soc. Am. **67**, 622.

Hayward, R. J., and B. R. Henry, 1976, Chem. Phys. **12**, 387.

Hayward, R. J., B. R. Henry, and W. Siebrand, 1973, J. Mol. Spectrosc. **46**, 207.

Henderson, J. R., M. Muramoto, T. M. Henderson, and J. B. Gruber, 1967, J. Chem. Phys. **47**, 5097.

Henry, B. R., 1977, Acc. Chem. Res. **10**, 207.

Henry, B. R., and W. Siebrand, 1968, J. Chem. Phys. **49**, 5369.

Heritage, J. P., J. G. Bergman, A. Pinzuk, and J. M. Worlock, 1979, "Picosecond Raman gain spectroscopy of cyanide on silver" (unpublished).

Hordvik, A., 1977, Appl. Opt. **16**, 2827.

Hordvik, A., and H. Schlossberg, 1977, Appl. Opt. **16**, 101.

Hordvik, A., and L. Skolnik, 1977, Appl. Opt. **16**, 2919.

Hu, C., and J. R. Whinnery, 1973, Appl. Opt. **12**, 72.

Hulbert, E. O., 1945, J. Opt. Soc. Am. **35**, 698.

Irvine, W. M., and J. B. Pollack, 1968, Icarus **8**, 324.

Kanstad, S. O., and P. E. Nordal, 1978, Opt. Commun. **26**, 367.

Kasoev, S. G., and L. M. Lyamshev, 1977, Akust. Zh. **23**, 890 (Sov. Phys.—Acoust. **23**, 510).

Kerr, E. L., 1973, Appl. Opt. **12**, 2520.

Kohanzadeh, Y., J. R. Whinnery, and M. M. Carroll, 1975, J. Acoust. Soc. Am. **57**, 67.

Kopelevich, O. V., 1976, Opt. Spektrosk. **41**, 666 [Opt. Spectrosc. (USSR) **41**, 391].

Kreuzer, L. B., 1971, J. Appl. Phys. **42**, 2934.

Kreuzer, L. B., and C. K. N. Patel, 1971, Science **173**, 45.

Lahmann, W., and H. J. Ludewig, 1977, Chem. Phys. Lett. **45**, 177.

Lahmann, W., H. J. Ludewig, and H. Welling, 1977, Anal. Chem. **49**, 549.

Landau, L. D., and E. M. Lifshitz, 1959, *Fluid Mechanics* translated from the Russian by J. B. Sykes and W. H. Reid (Pergamon, New York), Chap. VIII.

Levine, B. F., and C. G. Bethea, 1979, "Ultrahigh sensitivity stimulated Raman gain spectroscopy" (unpublished).

Long, M. E., R. L. Swofford, and A. C. Albrecht, 1976, J. Chem. Phys. **65**, 179.

Lyamshev, L. M., and K. A. Naugol'nykh, 1976, Akust. Zh. **22**, 625 (Sov. Phys.—Acoust. **22**, 354).

McClelland, J. F., and R. N. Kniseley, 1976, Appl. Opt. **15**, 2658; 2967.

McDavid, J. M., K. L. Lee, S. S. Yee, and M. A. Afromowitz, 1978, J. Appl. Phys. **49**, 6112.
McDonald, F. A., and G. C. Wetsel, Jr., 1978, J. Appl. Phys. **49**, 2313.
McQueen, D. H., 1979, J. Phys. D **12**, 1673.
Merkle, L. D., and R. C. Powell, 1977, Chem. Phys. Lett. **46**, 303.
Monahan, E. M., and A. W. Nolle, 1977, J. Appl. Phys. **48**, 3519.
Moses, E. I., and C. L. Tang, 1977, Opt. Lett. **1**, 115.
Naugol'nykh, K. A., 1977, Akust. Zh. **23**, 171 (Sov. Phys.—Acoust. **23**, 98).
Nechaev, S. Yu., and Yu. N. Ponomarev, 1975, Kvant. Elektron. (Moscow) **2**, 1400 (Sov. J. Quantum Electron. **5**, 752).
Nelson, E. T., and C. K. N. Patel, 1981, Opt. Lett. (in press).
Nordal, P. E., and S. O. Kanstad, 1977, Opt. Commun. **22**, 185.
Oda, S., T. Sawada, and H. Kamada, 1978, Anal. Chem. **50**, 865.
Palmer, R. A., J. C. Roark, and J. C. Robinson, "Photoacoustic detection of natural circular dichroism in crystalline transition metal complexes," in ACS Symposium entitled "The Stereochemistry of Optically Active Compounds of Transition Metals," (to be published).
Pao, Y. H., 1977, editor, *Optoacoustic Spectroscopy and Detection* (Academic, New York).
Parker, J. G., 1973, Appl. Opt. **12**, 2974.
Parker, J. G., and D. N. Ritke, 1973, J. Chem. Phys. **59**, 3713.
Patel, C. K. N., 1978, Science **202**, 157.
Patel, C. K. N., and R. J. Kerl, 1977, Appl. Phys. Lett. **30**, 578.
Patel, C. K. N., and A. C. Tam, 1979a, Appl. Phys. Lett. **34**, 467.
Patel, C. K. N., and A. C. Tam, 1979b, Chem. Phys. Lett. **62**, 511.
Patel, C. K. N., and A. C. Tam, 1979c, Appl. Phys. Lett. **34**, 760.
Patel, C. K. N., and A. C. Tam, 1979d, Nature **280**, 302.
Patel, C. K. N., and A. C. Tam, 1979e, "Pulsed opto-acoustic spectroscopy of liquids," in *Proceedings of the 4th International Conference on Laser Spectroscopy, Rottach-Egern, West Germany.*
Patel, C. K. N., and A. C. Tam, 1980, Appl. Phys. Lett. **36**, 7.
Patel, C. K. N., and A. C. Tam, and R. J. Kerl, 1979, J. Chem. Phys. **71**, 1470.
Pouch, J. J., R. L. Thomas, Y. H. Wong, J. Schuldies, and M. Srinivasan, 1979, "Scanning photoacoustic microscopy," in Technical Digest, Topical Meeting on Photoacoustic Spectroscopy, Ames, Iowa (unpublished).
Querry, M. R., P. A. Cary, and R. C. Waring, 1978, Appl. Opt. **17**, 3587.
Quimby, R. S., P. M. Selzer, and W. M. Yen, 1977, Appl. Opt. **16**, 2630.
Quimby, R. S., and W. M. Yen, 1978, Opt. Lett. **3**, 181.
Razumova, T. K., and I. O. Starobogatov, 1977, Opt. Spekrosk. **42**, 489 [Opt. Spectrosc. (USSR) **42**, 274].
Reddy, K. V., R. G. Bray, and M. J. Berry, 1978, in *Advances in Laser Chemistry*, edited by A. Zewail (Springer-Verlag, Berlin), p. 48.
Rentzepis, P. M., and Y. H. Pao, 1966, J. Chem. Phys. **44**, 2931.
Robin, M. B., 1976, J. Lumin. **13**, 131.
Robin, M. B., and N. A. Kuebler, 1975, J. Am. Chem. Soc. **97**, 4822.
Robin, M. B., and N. A. Kuebler, 1977, J. Chem. Phys. **66**, 169.
Rockley, M. G., and J. P. Devlin, 1977, Appl. Phys. Lett. **31**, 24.
Rockley, M. G., and K. M. Waugh, 1978, Chem. Phys. Lett. **54**, 597.
Rosencwaig, A., 1973, Opt. Commun. **7**, 305.
Rosencwaig, A., 1975, Anal. Chem. **47**, 592A.
Rosencwaig, A., 1977, Rev. Sci. Instrum. **48**, 1133.
Rosencwaig, A., 1978, Adv. Electron. and Electron Phys. **46**, 207.
Rosencwaig, A., and A. Gersho, 1976, J. Appl. Phys. **47**, 64.
Rosencwaig, A., J. L. Opsal, and J. F. Scheimer, 1979, "Photoacoustic Stress," in Technical Digest, Topical Meeting on Photoacoustic Spectroscopy, Ames, Iowa (unpublished).
Sam, C. L., and M. L. Shand, 1979, Opt. Commun. **31**, 174.
Shaw, R. W., 1979, Appl. Phys. Lett. **35**, 253.
Sigrist, M. K., and F. K. Kneubühl, 1978, J. Acoust. Soc. Am. **64**, 1652.
Sladky, P., R. Danielius, V. Sirutkaitis, and M. Boudys, 1977, Czech. J. Phys. **B27**, 1075.
Somoano, R. B., 1978, Angew. Chem. Int. Ed. Engl. **17**, 238.
Starobogatov, I. O., 1977, Opt. Spektrosk. **42**, 304 [Opt. Spectrosc. (USSR) **42**, 172].
Stone, J., 1978, Appl. Opt. **17**, 2876.
Sullivan, S. A., 1963, J. Opt. Soc. Am. **53**, 962.
Tam, A. C., and C. K. N. Patel, 1979a, Nature **280**, 304.
Tam, A. C., and C. K. N. Patel, 1979b, Appl. Opt. **18**, 3348.
Tam, A. C., and C. K. N. Patel, 1979c, Appl. Phys. Lett. **35**, 843.
Tam, A. C., C. K. N. Patel, and R. J. Kerl, 1979, Opt. Lett. **4**, 81.
Tam, A. C. and C. K. N. Patel, 1980, Opt. Lett. **5**, 27.
Tam, A. C. and Y. H. Wong, 1980, Appl. Phys. Lett. **36**, 471.
Teslenko, V. S., 1977, Kvant. Elektron. (Moscow) **4**, 1732 (Sov. J. Quantum Electron. **7**, 981).
Voigtman, E., A. Jurgensen, and J. Winefordner, 1981, Anal. Chem. (in press).
Von Gutfeld, R. J., and H. F. Budd, 1979, Appl. Phys. Lett. **34**, 617.
Wang, T. T., J. M. McDavid, and S. S. Yee, 1979, Appl. Opt. **18**, 2354.
Westervelt, P. J., and R. S. Larson, 1973, J. Acoust. Soc. Am. **54**, 121.
Wetsel, G. C., Jr., and F. A. McDonald, 1977, Appl. Phys. Lett. **30**, 252.
Wetsel, G. C., Jr., and F. A. McDonald, 1979, "Piezoelectric detection of photoacoustic signals," in Technical Digest, the Topical Meeting on Photoacoustic Spectroscopy, Ames, Iowa (unpublished).
White, R. M., 1963, J. Appl. Phys. **34**, 3559.
Wickramasinghe, H. K., R. C. Bray, V. Jipson, C. E. Quate, and J. R. Salcedo, 1978, Appl. Phys. Lett. **33**, 923.
Wilson, E. B., Jr., 1934, Phys. Rev. **45**, 706.
Wong, Y. H., R. L. Thomas, and G. F. Hawkins, 1978, Appl. Phys. Lett. **32**, 538.
Wunsch, L., H. J. Neusser, and E. W. Schlag, 1975a, Chem. Phys. Lett. **31**, 433.
Wunsch, L., H. J. Neusser, and E. W. Schlag, 1975b, Chem. Phys. Lett. **32**, 210.

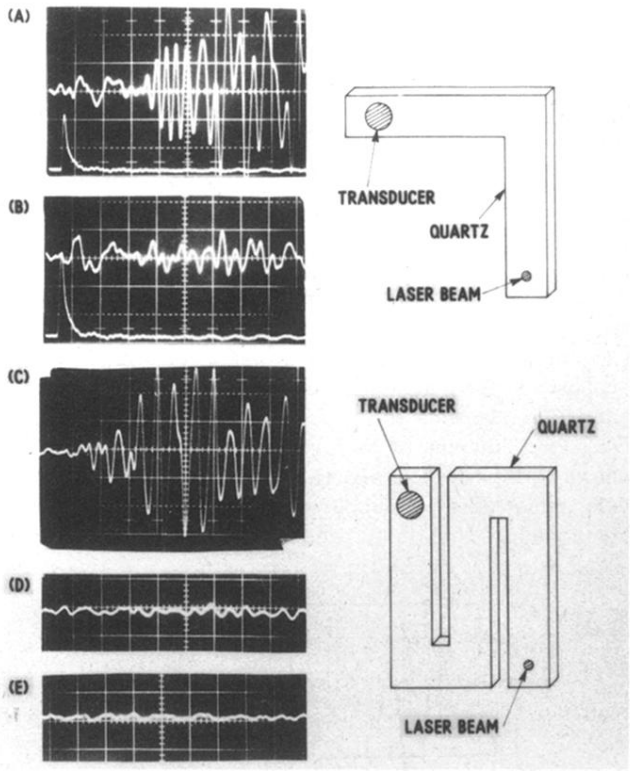

FIG. 11. Comparisons of two geometries for optoacoustic spectroscopy of powders. (A) and (C) show optoacoustic signals when the dye laser is tuned to the peak of an absorption line (no. 7) of Ho_2O_3 and (B) and (D) show corresponding signals when the dye laser is tuned away from the absorption peak. (E) shows the optoacoustic transducer output when the laser beam is blocked.

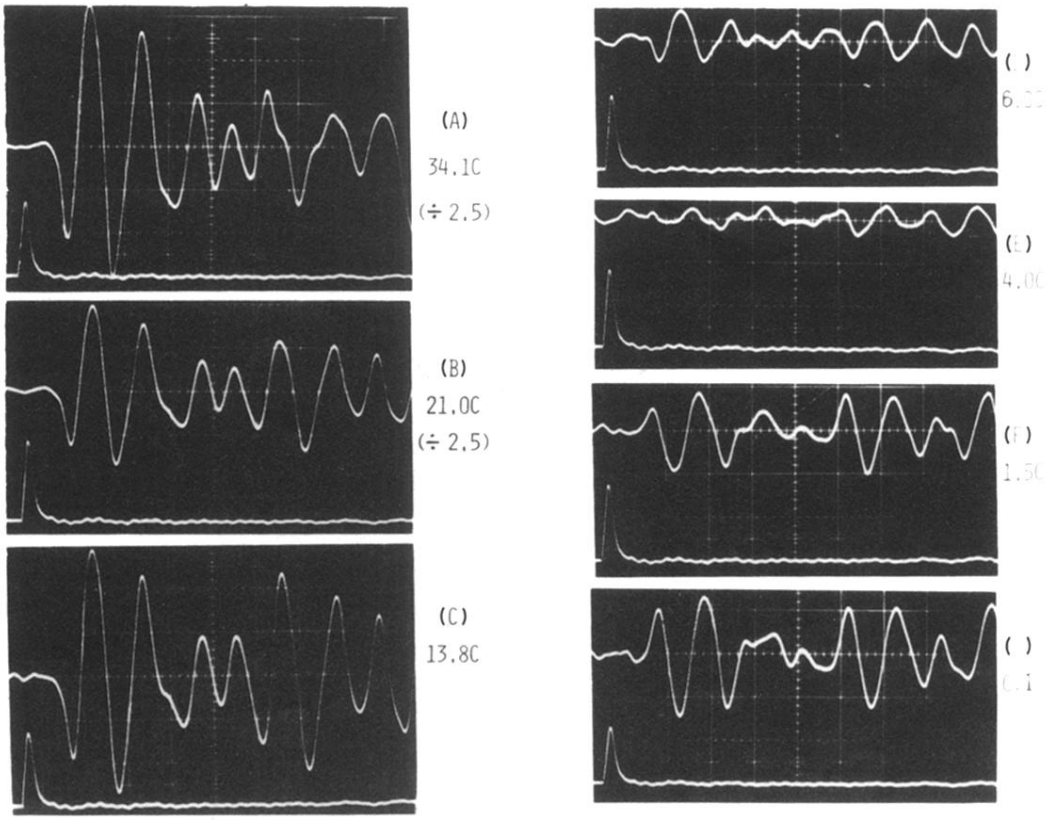

FIG. 13. Transducer output signal for water at various temperatures. In each of the scope pictures, the upper trace is the transducer output signal for liquid H_2O at the indicated temperature (in °C); the lower trace is the laser pulse detected by the pyroelectric detector. The laser frequency is fixed at 16 400 cm^{-1}. Horizontal scale is 5 μsec cm^{-1}. Vertical sensitivities are the same for all the pictures except (A) and (B), where the normal sensitivity is decreased by a factor of 2.5, as indicated. Note the phase reversal of the early part of the transducer output at 4 °C.

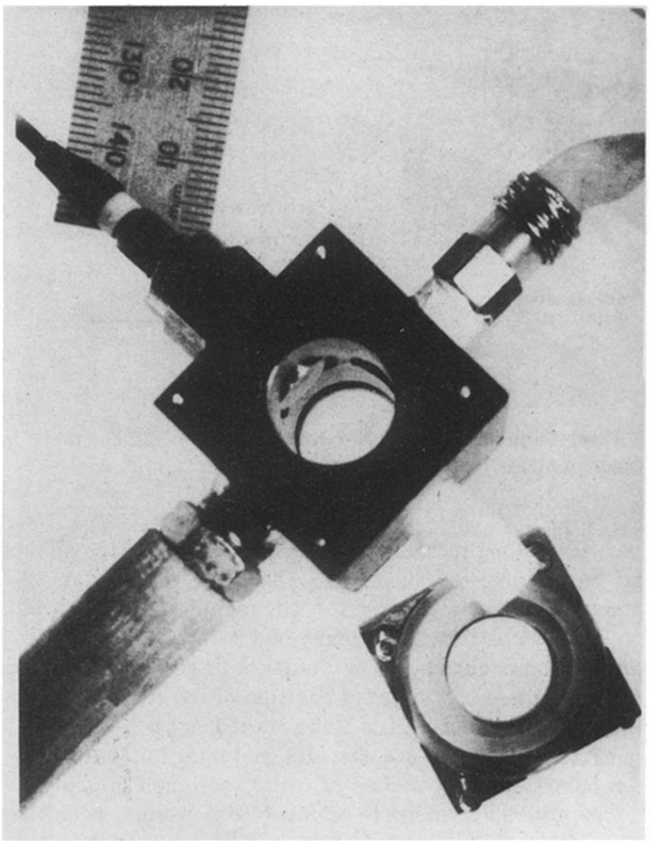

FIG. 5. Photograph of the stainless steel OA cell with a flange containing a quartz window removed. The polished transducer front diaphragm protruding into the cell can be clearly seen.